Molecular characteristics and diurnal variations of organic aerosols at a rural site in the North China Plain with implications for the influence of regional biomass burning

Jianjun Li[1,4], Gehui Wang[1,2,3 *], Qi Zhang[4*], Jin Li[1], Can Wu[2], Wenqing Jiang[4], Tong Zhu[5], and Limin Zeng[5]

[1]Key Lab of Aerosol Chemistry & Physics, SKLLQG, Institute of Earth Environment, Chinese Academy of Sciences, Xi'an 710061, China
[2]Key Laboratory of Geographic Information Science of the Ministry of Education, School of Geographic Sciences, East China Normal University, Shanghai 200241, China
[3]Institute of Eco-Chongming, 3663 N. Zhongshan Rd., Shanghai 200062, China
[4]Department of Environmental Toxicology, University of California, Davis, CA 95616, USA
[5]BIC-ESAT and SKL-ESPC, College of Environmental Sciences and Engineering, Peking University, Beijing, China

*Corresponding authors:
Prof. Gehui Wang, E-mail: ghwang@geo.ecnu.edu.cn;
Prof. Qi Zhang, E-mail: dkwzhang@ucdavis.edu

Abstract

Field burning of crop residue in early summer releases into the atmosphere a large amount of pollutants with significant impacts on the air quality and aerosol properties in the North China Plain (NCP). In order to investigate the influence of this regional anthropogenic activity on molecular characteristics of organic aerosol, we collected $PM_{2.5}$ filter samples every 3 hours at a rural site of NCP during June 10th to 25th, 2013, and analyzed them for more than 100 organic tracer compounds, including both primary (*n*-alkanes, fatty acids/alcohols, sugar compounds, polycyclic aromatic hydrocarbons, hopanes, and phthalate esters) and secondary (phthalic acids, isoprene-, α-/β-pinene, β-caryophyllene, and toluene-derived products) organic aerosol tracers, as well as for organic carbon (OC), elemental carbon (EC), and water-soluble organic carbon (WSOC). Total concentrations of the measured organics ranged from 177 to 6248 ng m^{-3} (mean 1806±1308 ng m^{-3}) during the study period, most of which were contributed by sugar compounds, followed by fatty acids and fatty alcohols. Levoglucosan (240±288 ng m^{-3}) was the most abundant single compound and strongly correlated with OC and WSOC, suggesting that biomass burning (BB) is an important source of summertime organic aerosols in this rural region. Based on analysis of fire spots and backward trajectories of air masses, two representative periods were classified, which are (1) Period 1 (P1), Jun 13th 21:00-16th 15:00, when air masses were uniformly from the southeast part of NCP, where intensive open-field biomass burning (BB) occurred and (2) Period 2 (P2), Jun 22nd 12:00-24th 06:00, which is representative of local emission. Nearly all the measured PM components showed much higher concentrations in P1 than in P2. Although *n*-alkanes, fatty acids,

and fatty alcohols presented similar temporal/diurnal variations as those of levoglucosan throughout the entire period, their molecular distributions were more dominated by high molecular weight (HMW) compounds in P1, demonstrating an enhanced contribution from BB emissions. In contrast, intensive BB emission in P1 seems to have limited influences on the concentrations of polycyclic aromatic hydrocarbons (PAHs), hopanes and phthalate esters. Both 3-hydroxyglutaric acid and β-caryophyllinic acid showed strong linearly correlations with levoglucosan (R^2=0.72 and 0.80, respectively), indicating that BB is also an important source for terpene-derived SOA formation. A tracer-based method was used to estimate the distribution of biomass-burning OC, fungal-spore OC and secondary organic carbon (SOC) derived from isoprene, α-/β-pinene, β-caryophyllene, and toluene in the different periods. The results showed that the contribution of biomass-burning OC to total OC in P1 (27.6%) was 1.7 times of that in P2 (17.1%). However, the contribution of SOC from oxidation of the four kinds of VOCs increased slightly from 16.3% in P1 to 21.1% in P2.

Key words: Organic aerosols; Molecular composition; North China Plain; Biomass Burning

1. Introduction

Organic aerosols (OA, i.e., the organic fraction of particles) constitute a substantial fraction (~10-90%) (Jimenez et al., 2009;Zhang et al., 2007a;Hallquist et al., 2009) of atmospheric particles, and have significant effects on global and regional climate (Venkataraman et al., 2005;Kanakidou et al., 2005), air quality (Aggarwal et al., 2013;Wang et al., 2006b), human health (Lelieveld et al., 2015), and ecosystems (Tie et al., 2016). Organic aerosols in the atmosphere can be emitted directly from various sources, such as combustion of fossil fuels, biomass burning, plant emission, and so on, which is defined as primary organic aerosols (POA). On the other hand, atmospheric secondary OA (SOA) are produced from photochemical oxidation products of volatile organic compounds (VOCs) via gas-particle conversion processes such as nucleation, condensation and heterogeneous chemical reactions (Hallquist et al., 2009). These organic species could modify physicochemical characteristics of atmospheric aerosols such as hygroscopicity, albedo, and oxidation state (Dinar et al., 2008;Chan et al., 2005;Fu et al., 2010). Thus, a thorough understanding of molecular composition and source of organic aerosols is necessary in order to address aerosol related environmental issues and to improve the accuracy of modelling studies.

Tremendous amounts of air pollutants including both particulate matters (PM) and their gaseous precursors (e.g., SO_2, NO_x, NH_3, and VOCs) are emitted into the atmosphere from power plants, industries and vehicles due to rapid economy development in China, leading to serious air conditions in the recent decades (Zhang et al., 2009;Guo et al., 2014;Wang et al., 2016;Huang et al., 2014;Li et al., 2017). The

North China Plain (NCP) has been recognized as one of the most polluted regions in the world, with very high concentrations of $PM_{2.5}$ on the ground surface (van Donkelaar et al., 2010). The NCP is also one of the most significant aerosol sources in the world, which has a significant impact on the East China Sea and Western North Pacific (Andreae and Rosenfeld, 2008). Thus, extensive efforts have been made in recent years to characterize the sources, properties, and processes of PM in the NCP. Most of these results concluded that the severe air pollution in the region is related to the source strength and frequently happens under stagnant weather conditions. Recently, it has been shown that the rapid growth of secondary aerosols could lead to an severe haze event in China under certain meteorological conditions (Wang et al., 2016;Sun et al., 2014;Quan et al., 2013).

In the rural area of NCP, biomass burning for domestic cooking and heating and agricultural waste disposal is an important source of atmospheric PM (Wang et al., 2009b;Li et al., 2010;Zhang et al., 2016). Particularly, the open-field burning is still a common way for disposal of crop residues (mainly wheat straw) in early summer (Li et al., 2007). This traditional activity could release huge amounts of pollutants into the atmosphere and significantly affect air quality and aerosol properties in the region. Zhu et al. (2016) examined the amounts of VOCs in the air at a rural site of Yucheng (Shandong Province, East China), and found that their concentrations during the wheat straw burning period are approximately twice of those in normal periods. Model results also revealed a significant influence of open burning of crop residual on ozone, CO, black carbon (BC) and organic carbon (OC) concentrations in NCP.

Moreover, both off-line (Fu et al., 2012;Wang et al., 2009b;Wang et al., 2011) and on-line (Sun et al., 2016) observations indicated that the intensive emission from wheat straw burning in the region could change the molecular distribution of organic aerosols of the downwind urban or mountain areas.

During June 10th to 25th of 2013, we conducted a continuous sampling campaign at a rural site in the northern part of NCP. $PM_{2.5}$ filter samples were collected with a 3-hour time resolution and determined for more than 100 organic compounds including aliphatic lipids, sugar compounds, hopanes, polycyclic aromatic hydrocarbons (PAHs), phthalate esters, and secondary oxidation products. The first objective of this study was to get an overall understanding of temporal/diurnal variation and molecular distribution of summertime OA in the rural region. The second objective was to compare the results in two representative periods to investigate the influence of regional field burning of wheat straw on the molecular characteristics of organic aerosols.

2. Experimental section

2.1 Sample collection

The sampling was performed at the Integrated Ecological-Meteorological Observation and Experiment Station of Chinese Academy of Meteorological Sciences (39°08’ N, 115°40’ E, 15.2 m asl), which is located in a rural area of Gucheng, Hebei Province. Detailed information of the station and sampling campaign was described in Li et al. (2018). Briefly, time-resolved (06:00–09:00, 09:00–12:00, 12:00–15:00, 15:00–18:00, 18:00–21:00, 21:00–24:00, 00:00–03:00, and 03:00–06:00, Beijing

time) $PM_{2.5}$ samples were collected on the rooftop (about 10 m above the ground) of a three-story building on the campus of the Gucheng station. The sampling was conducted by using a high volume (1.13 m^3 min^{-1}) sampler (Anderson) with a $PM_{2.5}$ inlet from June 10^{th} to 25^{th}, 2013. This period was chosen, because open-field burning of wheat straw in NCP mainly occur in the mid of June. All samples were collected onto pre-baked (450 °C, 6-8 hr) quartz fiber filters. Field blank samples were also collected by mounting blank filters onto the sampler for about 15 min without pumping any air. After sampling, the sample filter was individually sealed in aluminum foil bags and stored in a freezer (−20 °C) prior to analysis.

2.2 Organic compounds determination

A size of 12.5-25 cm^2 of the filter sample was cut and extracted with a mixture of dichloromethane and methanol (2:1, v/v) under ultrasonication. The extracts were concentrated using a rotary evaporator under vacuum conditions and then blow down to dryness using pure nitrogen. After reaction with N,O-bis-(trimethylsilyl) trifluoroacetamide (BSTFA) at 70 ℃ for 3 hrs., the derivatives were determined using gas chromatography/electron ionization mass spectrometry (GC/EI-MS) (Li et al., 2013b).

GC/EI-MS analysis of the derivatized fraction was performed using an Agilent 7890A GC coupled with an Agilent 5975C MSD. The GC separation was carried out on a DB-5MS fused silica capillary column with the GC oven temperature programmed from 50℃ (2 min) to 120℃ at 15℃ min^{-1} and then to 300℃ at 5℃ min^{-1} with a final isothermal hold at 300℃ for 16 min. The sample was injected in a

158 splitless mode at an injector temperature of 280℃, and scanned from 50 to 650
159 Daltons using electron impact (EI) mode at 70 eV.
160 GC/EI-MS response factors of all the target compounds were determined using
161 authentic standards except several isoprene-derived SOA tracers. Response factors of
162 isoprene-derived SOA tracers were substituted by those of related surrogated
163 standards, which were described in Li et al. (2018). No significant contamination
164 (<5% of those in the samples) was found in the blanks. Recoveries of all the target
165 compounds ranged from 80% to 120%. Data presented were corrected for the field
166 blanks but not corrected for the recoveries.
167 **2.3 OC, EC, and WSOC analysis**
168 OC (organic carbon) and EC (elemental carbon) were analyzed using DRI Model
169 2001 Carbon Analyzer following the Interagency Monitoring of Protected Visual
170 Environments (IMPROVE) thermal/optical reflectance (TOR) protocol. A size of
171 0.526 cm^2 sample filter was placed in a quartz boat inside the analyzer and stepwise
172 heated to temperatures of 140 ℃ (OC1), 280 ℃ (OC2), 480 ℃ (OC3), and
173 580 ℃ (OC4) in a non-oxidizing helium (He) atmosphere, and 580 ℃ (EC1),
174 740 ℃ (EC2), and 840 ℃ (EC3) in an oxidizing atmosphere of 2% oxygen in
175 helium. Pyrolyzed carbon (PC) is determined by reflectance and transmittance of 633
176 nm light. One sample was randomly selected from every 10 samples and re-analyzed.
177 Differences determined from the replicate analyses were <5% for TC, and <10% for
178 OC and EC.
179 Another aliquot of filter sample was extracted with organic-free Milli-Q water

under ultrasonication (15 min each, repeated 3 times) and filtered through a PTFE filter to remove any particles and filter debris. Then the water-extract was analyzed for water-soluble organic carbon (WSOC) using a TOC analyzer (TOC-L CPH, Shimadzu, Japan). The difference between OC and WSOC was considered as water-insoluble OC (WIOC). All carbonaceous components data reported here were corrected by the field blanks.

3. Results and discussion

3.1 Fire spots and air masses

At present, open-field burning is still a common activity for disposal of crop residue in the rural area of the North China Plain, especially during wheat harvest period from the end of May to the middle of June (Fu et al., 2012). These extensive emissions from regional biomass burning in the provinces of Anhui, Jiangsu, Shandong, Henan and Hebei in NCP can cause severe air pollution on a local and regional scale. In our previous study, the fire spots in NCP during the sampling period were provided based on the NASA satellite observation (https://firms.modaps.eosdis.nasa.gov/firemap/). Combining with information on air mass back-trajectories (http://ready.arl.noaa.gov/HYSPLIT.php), the sampling period was divided into two sections: (1) June 10-18, when air masses were mainly transported via long distances from the southeast part of NCP, where intensive emissions from wheat straw burning occurred; (2) June 19-25, when air masses were mostly influenced by local emissions and regional emission from biomass burning decreased dramatically (Li et al., 2018). In this study, we further selected two representative periods to estimate the contribution

of regional biomass burning. Period 1 (P1) designates 13th Jun 21:00 pm to 16th Jun 15:00 pm, during which air masses were influenced by intensive biomass burning and transported uniformly from the southeast part of NCP (Figure 1 a and b, and Figure S1). Period 2 (P2) designates 22nd Jun 12:00 pm to 24th Jun 06:00 am, during which fire spots in the regions were relatively scarce and air masses came predominantly from the surrounding areas of the sampling site (Figure 1 c and d). In addition, there were several intermittent rainfalls during June 20-22, which are favorable for wet deposition of atmospheric pollutants. Thus, aerosols collected in P2 are well representative of local fresh emission. It is worthwhile to note that the two samples collected during 21st June 18:00-24:00 pm were excluded from P2, because they were highly affected by near-site biomass burning emission (detailed information is provided in Section 3.3).

3.2 Concentrations of $PM_{2.5}$, OC, EC, WSOC and WIOC

Concentrations of $PM_{2.5}$ and carbonaceous components are presented in Table 1. $PM_{2.5}$ concentrations ranged from 21 to 395 μg m^{-3} with a mean value at 159±89 μg m^{-3} during the whole sampling period. As shown in Figure 2, $PM_{2.5}$ concentrations in P1 (average ± 1σ = 231±89 μg m^{-3}) increased continuously from around 150 μg m^{-3} to higher than 300 μg m^{-3}, indicating the occurrence of a severe air pollution episode. In contrast, $PM_{2.5}$ concentration during P2 is as low as 43±14 μg m^{-3}. Similarly, the average concentration of OC is 29.4±7.8 μg m^{-3} in P1, which is more than 5 time higher than that in P2 (5.5±1.7 μg m^{-3}) . EC concentrations also decreased dramatically from P1 (12.1±4.0 μg m^{-3}) to P2 (1.5±1.5 μg m^{-3}). The average OC/EC ratio is 3.0±0.9 for the whole sampling period, but the ratio was

higher in P2 (3.8±1.0) than in P1 (2.5±0.4), mainly due to the high SOA formation activities in the rural areas of NCP in summer. It's worthwhile to note that the average OC/EC ratio during the BB-influenced P1 is much lower than the results reported for wheat straw burning in combustion chamber (12.9 ± 2.1) (Tian et al., 2017) or residential stove (6.3-11.1) (Li et al., 2009). The first reason is that fossil fuel burning (such as coal burning and vehicle exhaust) with lower OC/EC ratio (Tian et al., 2017) are still important sources in the region, which are also discussed in Section 3.4. On the other hand, this phenomenon may also be related to different combustion conditions of agricultural residuals in the open field. Li et al. (2009) found that the flaming fire from biomass burning would result in more EC emission and lower OC/EC ratio compared to smoldering fire. Actually, Hays et al. (2005) obtained similar low OC/EC ratio of 2.4 for open wheat straw burning smoke from Washington, US. Thus, the lower ratio of OC/EC observed in this work may indicate that wheat straw combustion in NCP during P1 occurred mainly in the flaming phase.

As shown in Figure 2 and 3, the concentrations of WSOC show a consistent temporal variation as those of OC (R^2=0.82), highlighting the fact that WSOC is an important fraction of OC in this region. In addition, the average ratio of WSOC/OC is higher during P1 (0.62±0.16) than during P2 (0.48±0.12), mainly due to enhanced emissions of water-soluble organic compounds (such as sugars, fatty alcohols/acids) from biomass burning during P1. Due to the removal effect of the intermittent raining, concentrations of water-insoluble OC in P2 (3.0±1.3 μg m^{-3}) are also much lower than those in P1 (10.3±4.4 μg m^{-3}).

246 The diurnal variation profiles of EC/OC and WSOC/OC are shown in Figure 4.
247 EC/OC is generally lower in daytime and the lowest value occurred during 12:00-
248 15:00 pm, mainly due to enhanced daytime formation of SOC. Previous studies have
249 shown that secondary organic aerosols are mainly composed of water-soluble
250 compounds, e.g., polyacids/polyalcohols and phenols (Kondo et al., 2007;Wang et al.,
251 2009a). However, these compounds can come from primary emissions as well,
252 especially from biomass burning (Shen et al., 2017;Fu et al., 2012). In this study, the
253 WSOC/OC presents lower value during daytime, especially in the afternoon when
254 photo-chemical oxidation is favorable. In addition, the diurnal variation pattern of
255 WSOC/OC is similar to that of levoglucosan/OC. Given that levoglucosan is a marker
256 of biomass burning emissions (Simoneit et al., 1999;Simoneit et al., 2004a), and many
257 SOA could be produced in the biomass burning plumes during the long-range
258 transport (detailed discussions are given in Section 3.3), these results indicate that
259 particulate WSOC in the region is mostly derived from biomass burning activities
260 including direct emission and secondary oxidation.

261 **3.3 Organic molecular composition**

262 More than 100 organic species were detected in the aerosol samples, and their
263 concentrations are shown in Table 2 and S1. In this study, these organic compositions
264 are grouped into 10 compound classes based on functional groups and sources. Total
265 concentrations of the measured organics ranged from 177 to 6248 ng m^{-3} (average =
266 1806$\pm$1308 ng m^{-3}) during the whole sampling period with the predominance of
267 sugar compounds, followed by fatty acids and fatty alcohols. The temporal variation

profiles of the determined organic groups are shown in Figure 5. Nearly all the measured organic species, especially *n*-alkanes, fatty acids, fatty alcohols, sugar compounds, and PAHs, show much higher concentrations in P1 than in P2 (Figure S2), indicating an important influence of regional biomass burning on airborne organic aerosols in NCP.

3.3.1 Biomass-burning tracers

As described in Section 3.1, intensive emissions of open biomass burning were observed in the southern part of NCP during June 13-16 (P1), which is an important reason for the severe regional air pollution during this period. Levoglucosan, which is produced in large quantities during pyrolysis of cellulose, is a key tracer for biomass burning emissions (Simoneit, 2002;Simoneit et al., 1999). As shown in Table 2, levoglucosan is the most abundant single compound in the whole sampling period, ranged from 5.6 to 1447 ng m^{-3} with a mean concentration of 240±288 ng m^{-3}. Levoglucosan shows good positive correlations with both OC (R^2=0.61) and WSOC (R^2=0.65) (Figure 3), confirming that biomass burning is an important source of both aerosol OC and WSOC in the rural region of NCP during the sampling period. As clearly shown in Figure 6, the concentrations of levoglucosan present a continual increasing trend during P1 with a mean value of 404±344 ng m^{-3}. However, the tracer presents very low concentrations (11-123 ng m^{-3}) for the most of time during Jun 20-22. Interestingly, the concentration of levoglucosan suddenly increased by more than 10 times at 21st Jun 18:00 pm to approximately 1200 ng m^{-3} within less than 3 hours and decreased to its beginning concentration (less than 100 ng m^{-3}) within 6 hours (2

290 samples) afterwards. The concentrations of OC, WSOC and EC also showed obvious
291 peaks during this event. However, based on analyses of back-trajectories (Figure 1c)
292 and wind conditions (Figure S1), we didn't find significant change of air mass origins.
293 Also, not all organic markers showed similar variation as levoglucosan. For example,
294 the concentrations of PAHs, hopanes, and phthalate esters changed little during this
295 event. Thus, it is plausible to conclude that this variation was caused by emissions
296 from biomass burning activities nearby the sampling site. For this reason, the data of
297 the 2 samples were excluded from P2.

298 The two isomers of levoglucosan, galactosan and mannosan, are also produced
299 by the pyrolysis of cellulose/hemicelluloses (Simoneit, 2002), and thus also
300 considered as important markers of biomass burning. Similar to levoglucosan, the
301 concentrations of these two anhydrosugars in P1 are 5-6 times higher than those in P2.
302 The isomeric ratios of levoglucosan to other anhydrosugars are considered as good
303 indicators of biomass burning. Fabbri et al. (2009) compared the concentrations of the
304 three anhydrosaccharides in the smokes from different fuel types, and proposed that
305 levoglucan/(galactosan+mannosan) (L/G+M) and levoglucan/mannosan (L/M) values
306 range in 0.2-18 and 0.23-33 for various source tests for biomass burning as compared
307 to the average of 54 and 54 for lignites. As shown in Table 2, average ratios of L/G+M
308 and L/M during P1 (10.1±3.41 and 6.77±1.97, respectively) and P2 (29.7±12.2 and
309 18.0±4.28) suggest that biomass burning is always the dominated contributor for
310 these compounds in the rural area of NCP in summer.

311 **3.3.2 Aliphatic lipid composition**

312 The average concentration of all the *n*-alkanes (C_{18}–C_{36}) measured in this study
313 is 207±149 ng m^{-3} with the most abundant individual compound being nonacosane
314 (C_{max}=$C_{29}H_{60}$) (Table S1). *n*-Alkanes derived from terrestrial plants are dominated by
315 high molecular weight species (HMW, carbon number >25) with an odd number
316 preference. In contrast, fossil fuel derived *n*-alkanes do not have odd/even number
317 preference (Rogge et al., 1993a;Simoneit et al., 2004b). In general, *n*-alkanes with a
318 carbon preference index (CPI, odd/even) more than 5 are considered as plant wax,
319 while those with a CPI nearly unity are mostly derived from fossil fuel combustion
320 (Rogge et al., 1993a, b). In this study, the mean value of CPI is 2.47±1.12, indicating
321 that both fossil fuel and plant wax contributed to *n*-alkanes in the rural areas of NCP
322 in summer. However, *n*-alkanes showed a stronger odd/even carbon number
323 predominance in P1 (CPI=2.85) than in P2 (CPI=1.64). In addition, all the low
324 molecular weight *n*-alkanes (LMW, carbon number <25) presented a higher
325 contribution to total *n*-alkanes in P2 than in P1 (Figure 7 a and d). These results
326 demonstrate that plant waxes from biomass burning emissions made a bigger
327 contribution to organic aerosols in the sampling region during P1.
328 A homologous series of 19 saturated fatty acids ($C_{12:0}$–$C_{32:0}$) and 3 unsaturated
329 fatty acids ($C_{16:1}$, $C_{18:1}$, and $C_{18:2}$) were detected in the samples (Table S1), and their
330 total concentration was 514±384 ng m^{-3} during the whole period. A strong even
331 carbon number predominance was observed with C_{max} at $C_{28:0}$ and $C_{16:0}$ (Table S1).
332 Higher molecular weight (HMW) fatty acids ($\geqslant C_{20}$) are derived from terrestrial plant
333 waxes, while LMW fatty acids ($\leqslant C_{19}$) have multiple sources such as vascular plants,

334 microbes and marine phytoplankton as well as kitchen emissions (Rogge et al.,
335 1993b;Kawamura et al., 2003). The total concentrations of fatty acids presented
336 similar temporal variation to levoglucosan with a robust linear correlation (R^2=0.72)
337 (Figure 8a), indicating that fatty acids are mostly affected by biomass burning
338 emission during the whole sampling period. Still, there are some evidences that
339 regional emission from wheat straw burning significantly affected the distribution of
340 fatty acids in the aerosols of Gucheng during P1. Firstly, the total concentrations of
341 fatty acids in P1 (900±358 ng m^{-3}) are more than 6 times higher than those in P2
342 (145±48 ng m^{-3}). Secondly, the concentrations and relative contributions of HMW
343 fatty acids ($C_{20:0}$–$C_{32:0}$) are much higher in P1 than in P2, similar to the results of *n*-
344 alkanes. In addition, the mean value of CPI of HMW fatty acids in P1 (4.21±1.14) is
345 also higher than that in P2 (3.50±1.64).

346 Fatty alcohols in the range of C_{22}–C_{30} were detected for the $PM_{2.5}$ samples with a
347 mean concentration of 193±187 ng m^{-3} (Table 2 and S1) during the whole sampling
348 period. Their distributions are characterized by even carbon number predominance
349 with a maximum at C_{28} (Figure 7c and f). The total concentration of fatty alcohols
350 strongly correlated with levoglucosan (R^2=0.73) (Figure 8b), suggesting that they can
351 also emitted from biomass burning. It is reasonable since HMW fatty alcohols ($\geqslant C_{20}$)
352 abundantly present in higher plants and loess deposits (Wang and Kawamura, 2005).
353 Similar to fatty acids, nearly 10 times higher concentration of fatty alcohols was
354 observed in P1 (322±151 ng m^{-3}) compared with those in P2 (34±23 ng m^{-3}).

355 **3.3.3 Primary saccharides**

In addition to the three anhydrosugars, 4 primary sugars (fructose, glucose, sucrose and trehalose) and 3 sugar alcohols (arabitol, mannitol and inositol) were detected in the samples. Primary saccharides have been used as biomarkers for primary biota emissions (Wang et al., 2011). Their mean concentrations ranged from 3.6 to 49 ng m^{-3} during the whole sampling period. In this study, concentrations of fructose, sucrose and trehalose in P1 were 7-10 times higher than those in P2 (Table S1). They well correlated with levoglucosan (R^2=0.47-0.62, Figure S3) during P1, in contrast to P2, during which no relationships were found between them. These results indicated that these primary sugars were also affected by open-field emissions of biomass burning during P1. Sugar alcohols, mainly arabitol and mannitol, are abundant in airborne fungal spores (Graham et al., 2002). Some studies suggested that biomass burning activities can enhance the emission of sugar alcohols at a certain level (Engling et al., 2009;Fu et al., 2012;Yang et al., 2012). However, no significant relationship (R^2<0.10) can be found between these sugar alcohols and levoglucosan even in P1, indicating the negligible contribution of biomass burning to the tracers in this study.

3.3.4 PAHs, Hopanes and Phthalates

As shown in Figure 5, the temporal variation of PAHs, hopanes, and phthalate esters were clearly different from those of the molecular tracers for biomass burning, especially in P1. In contrast to the continuous increase of sugars, fatty acids, fatty alcohols, and n-alkanes during P1, the concentration of PAHs, hopanes, and phthalate esters showed obvious day-night variations, indicating that biomass burning activities contributed little on these species. Phthalates are widely used as plasticizers in synthetic

polymers or softeners in polyvinylchlorides (PVC) (Simoneit et al., 2004b) and can be directly emitted from the matrix into the air as they are not chemically bonded with the matrix. Six phthalate esters were detected in the sampling aerosols, i.e., dimethyl (DMP), diethyl (DEP), diisobutyl (DiBP), butyl isobutyl (BiBP), di-n-butyl (DnBP), and bis(2-ethylhexyl) (BEHP) phthalates (Table S1). The concentrations of total detected phthalate esters in P1 (112±33 ng m^{-3}) are around 2 times only higher than those in P2 (51±18 ng m^{-3}). Hopanes are abundant in coal and crude oils and enriched in lubricant oil fraction (Oros and Simoneit, 2000;Kawamura et al., 1995).They can be emitted to the atmosphere from coal burning and/or internal combustion of fuel in engines. Only two dominant hopanes, 17α(H),21β(H)-30-norhopane($C_{29\alpha\beta}$) and 17α(H),21β(H)-hopane($C_{30\alpha\beta}$), were detected in all of the samples in this study. Their average concentration in P1 (4.40±2.48 ng m^{-3}) is ~ 2.5 times of that in P2 (1.81± 0.31 ng m^{-3}). Considering the much higher concentrations of levoglucosan in P1 (on average ~ 8 times higher than P2), these results again confirmed a limited influence of biomass burning on concentrations of phthalate esters and hopanes in the aerosols in the rural region. Thus, there were no significant concentration changes of the two species at 21st Jun 18:00-24:00 pm, when the air masses were highly affected by nearby biomass burning activities.

PAHs are the products of incomplete combustion of carbon-containing materials and are of high toxicity and carcinogenicity (Halek et al., 2008;Sultan et al., 2001). Previous studies indicated that PAHs are mainly emitted from coal burning and vehicle exhaust in most areas of China (Wang et al., 2006a). However, it has been reported that

400 combustion of biomass materials can also contribute to the PAHs in the atmosphere
401 (Simoneit, 2002;Ge et al., 2012;Young et al., 2016). In this study, PAH has no
402 significant correlation with levoglucosan during the whole sampling period. Yet the
403 concentrations of total PAHs in P1 (18.6±11 ng m^{-3}) are nearly 8 times higher than
404 those in P2 (2.3±1.0 ng m^{-3}). These results mean that although the emission of biomass
405 burning is not the most important source for PAHs during the entire period, the intensive
406 regional burning of wheat straw in P1 can also enhance the PAHs concentration in the
407 atmosphere of Gucheng.

408 As shown in Figure 9, all the primary aerosol markers mentioned above showed
409 lower concentrations in daytime with lowest concentrations at afternoon (12:00-18:00
410 pm), in consistent with the favorable dispersion conditions caused by high temperature
411 and planetary boundary layer (PBL) height. However, the day-night variation of PAHs,
412 hopanes, and phthalate esters are more obvious than other species, again confirming the
413 lower contribution of biomass burning to these organic compositions.

414 **3.3.5 Secondary organic aerosols (SOA) tracers**

415 Eight compounds were identified as isoprene oxidation products in the $PM_{2.5}$
416 samples, including two methyltetrahydrofuran diols, three C_5-alkene triols, two 2-
417 methyltetrols, and 2-methylglyceric acid (Table S1). Detailed information about
418 formation and contribution of these compositions were discussed in our previous paper
419 (Li et al., 2018). The concentrations of total detected isoprene-derived products are 112
420 ±86 ng m^{-3}, with much higher concentration in P1 (209±105 ng m^{-3}) than in P2 (57
421 ±29 ng m^{-3}).

cis-Pinonic acid (PNA), pinic acid (PA), 3-hydroxyglutaric acid (HGA) and 3-methyl-1,2,3-butanetricarboxylic acid (MBTCA) were detected as tracers for α-/β-pinene oxidation in this study, and their concentration are shown in Table S1. The concentration of total detected α-/β-pinene oxidation tracers is 66±31 ng m^{-3}, with MBTCA (31±14 ng m^{-3}) being the major compound during the whole sampling period. PNA and PA are considered as first-generation products of α-/β-pinene oxidation. They can be produced by further oxidation of carbonyl-substituted Criegee intermediates formed by α-pinene ozonolysis (Jenkin et al., 2000;Ma et al., 2008), or by OH oxidation of α-pinene under NO_x free conditions (Eddingsaas et al., 2012;Xuan et al., 2015). The formation of 3-HGA is supposed to be based on a ring opening mechanism and may be related to a heterogeneous reaction of these monoterpenes with irradiation in the presence of NOx (Jaoui et al., 2005;Claeys et al., 2007). As shown in Figure 6b-d, PNA, PA and HGA present similar temporal variations and correlated well each other (R^2=0.48-0.76, Figure S4). The formation of MBTCA is explained by further photodegradation of *cis*-pinonic acid and pinic acid with OH radical (Müller et al., 2012;Szmigielski et al., 2007). As a later-generation oxidation products, MBTCA showed an obviously different temporal variation profile than those of PNA and PA, and had no significant increase during P1. In addition, the concertation of PNA, PA and HGA in P1 are 2-8 times higher than those in P2. However, the concentrations of MBTCA in the two periods are comparable. These results are consistent with the longer time scales of formation pathway, lower volatility and longer lifetime of MBTCA in the atmosphere compared to the first-generation products of α-/β-pinene oxidation. β-

Caryophyllinic acid, formed either by ozonolysis or photo-oxidation of β-caryophyllene (a sesquiterpene) (Jaoui et al., 2007), was also determined in this study, and its concentration ranged from 0.49 to 78 ng m^{-3} (Ave. 17±17 ng m^{-3}). The mean concentration of β-caryophyllinic acid in P1 is 35±21 ng m^{-3}, being 5 times higher than that in P2 (4.1±1.2 ng m^{-3}).

Undoubtedly, the combustion of biomass materials can release a large amount of volatile organic compounds, including isoprene and terpenoids (Andreae and Merlet, 2001). As shown in Figure 5 and 6, the total biogenic SOA tracers, the sum of detected tracers of isoprene, α-/β-pinene, and β-caryophyllene derived SOA, showed a similar temporal variation pattern as levoglucosan with a moderate correlation (R^2=0.56, Figure S5a). Specifically, levoglucosan showed strong linearly correlations with 3-hydroxyglutaric acid (R^2=0.72) (Figure 8c) and β-caryophyllinic acid (R^2=0.80) (Figure 8d), indicating a significant contribution of biomass burning emissions to the formation of SOA derived from mono- and sesqui- terpene oxidation. In our previous paper (Li et al., 2018), we discussed the different diurnal variations of isoprene-derived SOA tracers. In this study, the diurnal variations of other SOA tracers are shown in Figure 10. All the SOA tracers presented weaker day-night variations compared to primary organic aerosol markers, because of the competition between the enhanced daytime formation by photoxidation and the nighttime accumulation associated with a low PBL. Yet, there are some differences between these SOA tracers. For example, PNA and PA presented lowest concentrations in the afternoon (12:00-18:00 pm) due to their relatively high volatilities, which is unfavorable for gas-to-particle phase partitioning. However, the

later-generation product of PNA and PA, i.e., the less volatile MBTCA, continuously increased during the daytime.

Two classes of aromatic SOA markers, phthalic acids and 2,3-dihydroxy-4-oxopentanoic acid (DHOPA), were detected in the samples as well. Phthalic acids are believed to be produced by the oxidation of naphthalene and other PAHs (Kawamura et al., 2005;Kawamura and Ikushima, 1993;Kanakidou et al., 2005). The mean concentrations of total phthalic acids in the whole sampling period ranged from 17 to 487 ng m^{-3} with a mean value of 155±94 ng m^{-3}. Their different temporal variation patterns than levoglucosan suggest that biomass burning emission contributes little to phthalic acids formation in the region. The DHOPA was considered to be a tracer compound for toluene-derived SOA (Kleindienst et al., 2004). DHOPA presented a similar temporal variation and moderate correlation to levoglusoan (R^2=0.51, Figure S5b), indicating a certain contribution of biomass burning. Similar to MBTCA, the volatility of DHOPA is quite low, and thus mainly exists in the particle phase at field temperature (Ding et al., 2017). Thus, DHOPA showed a similar diurnal variation to MBTCA, with higher concentrations during daytime.

3.4 Assessment of source contributions

In order to investigate the differences in organic aerosol sources between the two representative periods, we classified all the measured organic compounds into seven different sources: (a) “plant emission” represented by higher plant wax n-alkanes, HMW fatty acids and fatty alcohols ($\geqslant C_{20}$); (b) “fossil fuel combustion” mainly represented by fossil fuel derived n-alkanes, hopanes, and PAHs; (c) “biomass burning”

488 represented by levoglucosan and its isomers; (d) "marine/microbial source" represented
489 by LMW fatty acids (<C_{20}); (e) "soil/fungal spore/pollen" represented by primary
490 saccharides and sugar alcohols; (f) "plastic emission" represented by phthalate esters;
491 and (g) "secondary oxidation" represented by biogenic SOA tracers, DHOPA, and
492 phthalic acids. The concentrations of individual classes and their contributions to OC
493 content during P1 and P2 are summarized in Figure 11. Plant emission-derived
494 compounds accounted for a larger fraction of $PM_{2.5}$ OC during P1 than during P2 (mean
495 fractions of 28.7 ± 9.3‰ in P1 vs. 16.5 ±7.2‰ in P2). The average faction of biomass
496 burning-derived organics in P1 was also higher in P1 than in P2 (6.0 ± 3.9‰ vs. 4.6 ±
497 2.1‰), so do organics derived from soil/fungal spore/pollen. However, organic
498 molecules from the other 4 sources presented a higher contribution to OC in P2 than in
499 P1.

500 Since organic compounds in the $PM_{2.5}$ samples cannot be completely determined
501 and some of them are of different sources, thus the above classification based on the
502 measured compounds could result in certain uncertainty in assessing source
503 contributions (Simoneit et al., 2004b). Here, we further used a tracer-based source
504 apportionment method to quantitatively estimate the contributions of primary and
505 secondary sources to the fine particulate OC at the rural site. As described above, two
506 samples collected at 21st Jun 18:00-24:00 pm were considered to be highly affected by
507 the direct emission from biomass burning nearby the sampling site. Thus, the average
508 OC/levoglucosan ratio in the smoke of biomass burning ($\left(\frac{OC}{Levo}\right)_{BB}$) can be estimated
509 by using the following equation:

$$\left(\frac{OC}{Levo}\right)_{BB} = \frac{OC_n - \frac{1}{2}(OC_{before} + OC_{after})}{Levo_n - \frac{1}{2}(Levo_{before} + Levo_{Levo})} \quad (E1)$$

where OC_n and $Levo_n$ are the average concentrations of OC and levoglucosan in the two $PM_{2.5}$ samples affected by the nearby sources. OC_{before} and $Levo_{before}$ are the concentrations of OC and levoglucosan in the samples collected before the event, while OC_{after} and $Levo_{after}$ are the concentrations of OC and levoglucosan in the samples collected after the event. The mean values in the "before" and the "after" samples were subtracted to minimize the influence of local background contribution. The calculated $\left(\frac{OC}{Levo}\right)_{BB}$ in this study is 18.7, which is somewhat higher than the average value of 12.1 measured in $PM_{2.5}$ aerosols emitted from the burning of three types of cereal straws (i.e., wheat, maize, and rice) in China (Zhang et al., 2007b). This difference can be attributed to the differences of burning conditions. For other sources, the measured concentrations of mannitol were used to calculate the contributions of fungal spores to OC (Bauer et al., 2008), and SOA tracers were used to estimate the SOC formed from the oxidation of isoprene, α-/β-pinene, β-caryophyllene, and toluene (Kleindienst et al., 2007). Also, these tracer-based approaches tend to have large uncertainties, especially for SOC estimation (Li et al., 2013a). However, our results are still meaningful to understand the relative abundances of organic aerosols from these sources in different periods.

As shown in Figure 12, biomass-burning derived OC, ranging from 0.11-27.5 μgC m^{-3}, is the dominant source, which accounts for 1.16-74.8% (ave. 22.6%) of OC in the aerosols of the rural region during the whole sampling period. Fungal-spore derived OC (0.003-5.12 μgC m^{-3}) is a minor source, only accounting for 0.43% (0.003-5.12%) of

OC. The contribution of total SOC derived from oxidation of isoprene, α-/β-pinene, β-caryophyllene, and toluene to OC ranged from 5.90-34.1% with an average at 16.7%. Among the four SOC precursors, toluene-derived products accounted for 7.78% (2.06-21.7%) of OC, being the most important SOC contributor. The relative abundances of these sources showed clear temporal variations during the whole sampling period (Figure 12). The contribution of biomass burning derived OC to total OC in P1 (27.6%) was 1.7 times of that in P2 (17.1%) (Figure 13), further indicating the strong regional impact of open-field wheat straw burning on the molecular compositions of organic aerosols in the rural area of NCP. The contribution of SOC from oxidation of the four VOCs increased slightly from P1 (16.3%) to P2 (21.1%). It should be noted that biomass burning can also release a large amount of VOCs, which may produce more secondary organic aerosols during the long-range transport. Thus, the impact of intensive biomass burning in the southern region of NCP on organic aerosols in the Gucheng area is likely even stronger than the estimation presented above with implications for regional climate.

4. Summary and Conclusion

During the entire sampling period, OC and WSOC showed strong positive correlations with levoglucosan, and the diurnal variation of WSOC/OC was similar to that of levoglucosan/OC, suggesting that summertime organic aerosols in the rural area of NCP are highly affected by direct emission of BB. Higher relative abundances and CPI values of HMW n-alkanes, fatty acids and fatty alcohols in P1 indicated an enhancing effect of open-field biomass burning on molecular composition of organic

aerosols. PAHs, hopanes, and phthalate esters presented different temporal and diurnal variations from levoglucosan because of the lower contribution of BB to these organic compositions. The total biogenic SOA tracers showed a similar temporal variation and a moderate correlation with levoglucosan, demonstrating the enhancing effect of BB emission on BSOA formation. Later-generation SOA products, e.g., MBTCA in this study, are unlikely affected directly by BB emission, and thus show little changes in concentrations between the two periods. The source distribution results derived using a tracer-based method demonstrated that the contribution of BB to organic aerosols increased by more than 50% during the period influenced by regional open-field biomass burning (P1) compared to the period when local emissions were more dominant (P2). However, this contribution may even be underestimated since BB can also release a large amount of VOCs enhancing the formation of SOA in the atmosphere. Our results confirmed that intensive field burning of biomass fuels can significantly influence the concentration and composition of aerosols, and thus affect atmospheric chemistry and climate on a regional scale.

Author Contributions

G.H. Wang designed the experiment. G.H. Wang, T. Zhu and L.M. Zeng arranged the sample collection. J.J. Li. and G.H. Wang collected the samples. J.J. Li, G.H. Wang, J. Li, C. Wu and W.Q. Jiang analyzed the samples. J.J. Li, and G.H. Wang performed the data interpretation. J.J. Li, G.H. Wang and Q. Zhang wrote the paper.

Acknowledgements

This work was financially supported by the program from National Nature Science Foundation of China (No. 41773117, 91543116, 41405122). The authors gratefully acknowledge the use of fire spots data products from the Land, Atmosphere Near real-time Capability for EOS (LANCE) system operated by the NASA/GSFC/Earth

Science Data and Information System (ESDIS) with funding provided by NASA/HQ (https://firms.modaps.eosdis.nasa.gov/firemap/), and the NOAA Air Resources Laboratory (ARL) for the provision of the HYSPLIT transport and dispersion model and/or READY website (http://www.ready.noaa.gov) used in this publication.

Reference

Aggarwal, S. G., Kawamura, K., Umarji, G. S., Tachibana, E., Patil, R. S., and Gupta, P. K.: Organic and inorganic markers and stable C-, N-isotopic compositions of tropical coastal aerosols from megacity Mumbai: sources of organic aerosols and atmospheric processing, Atmos. Chem. Phys., 13, 4667-4680, 10.5194/acp-13-4667-2013, 2013.

Andreae, M. O., and Merlet, P.: Emission of trace gases and aerosols from biomass burning, Global Biogeochemical Cycles, 15, 955-966, 10.1029/2000gb001382, 2001.

Andreae, M. O., and Rosenfeld, D.: Aerosol–cloud–precipitation interactions. Part 1. The nature and sources of cloud-active aerosols, Earth-Science Reviews, 89, 13-41, 10.1016/j.earscirev.2008.03.001, 2008.

Chan, M. N., Choi, M. Y., Ng, N. L., and Chan, C. K.: Hygroscopicity of water-soluble organic compounds in atmospheric aerosols: Amino acids and biomass burning derived organic species, Environ. Sci. Technol., 39, 1555-1562, 10.1021/es049584l, 2005.

Claeys, M., Szmigielski, R., Kourtchev, I., Van der Veken, P., Vermeylen, R., Maenhaut, W., Jaoui, M., Kleindienst, T. E., Lewandowski, M., Offenberg, J. H., and Edney, E. O.: Hydroxydicarboxylic Acids: Markers for Secondary Organic Aerosol from the Photooxidation of α-Pinene, Environ. Sci. Technol., 41, 1628-1634, 10.1021/es0620181, 2007.

Dinar, E., Anttila, T., and Rudich, Y.: CCN activity and hygroscopic growth of organic aerosols following reactive uptake of ammonia, Environ. Sci. Technol., 42, 793-799, 10.1021/es071874p, 2008.

Ding, X., Zhang, Y. Q., He, Q. F., Yu, Q. Q., Wang, J. Q., Shen, R. Q., Song, W., Wang, Y. S., and Wang, X. M.: Significant Increase of Aromatics-Derived Secondary Organic Aerosol during Fall to Winter in China, Environ. Sci. Technol., 51, 7432-7441, 10.1021/acs.est.6b06408, 2017.

Eddingsaas, N. C., Loza, C. L., Yee, L. D., Chan, M., Schilling, K. A., Chhabra, P. S., Seinfeld, J. H., and Wennberg, P. O.: alpha-pinene photooxidation under controlled chemical conditions - Part 2: SOA yield and composition in low- and high-NOx environments, Atmos. Chem. Phys., 12, 7413-7427, 10.5194/acp-12-7413-2012, 2012.

Engling, G., Lee, J. J., Tsai, Y. W., Lung, S. C. C., Chou, C. C. K., and Chan, C. Y.: Size-Resolved Anhydrosugar Composition in Smoke Aerosol from Controlled Field Burning of Rice Straw, Aerosol Science and Technology, 43, 662-672, 10.1080/02786820902825113, 2009.

Fabbri, D., Torri, C., Simoneit, B. R. T., Marynowski, L., Rushdi, A. I., and Fabiańska, M. J.: Levoglucosan and other cellulose and lignin markers in emissions from burning of Miocene lignites, Atmos. Environ., 43, 2286-2295, 2009.

Fu, P. Q., Kawamura, K., Pavuluri, C. M., Swaminathan, T., and Chen, J.: Molecular characterization of urban organic aerosol in tropical India: contributions of primary emissions and secondary photooxidation, Atmos. Chem. Phys., 10, 2663-2689, 2010.

Fu, P. Q., Kawamura, K., Chen, J., Li, J., Sun, Y. L., Liu, Y., Tachibana, E., Aggarwal, S. G., Okuzawa, K., Tanimoto, H., Kanaya, Y., and Wang, Z. F.: Diurnal variations of organic molecular tracers and stable carbon isotopic composition in atmospheric aerosols over Mt. Tai in the North China Plain: an influence of biomass burning, Atmos. Chem. Phys., 12, 8359-8375, 10.5194/acp-12-8359-2012, 2012.

Ge, X., Setyan, A., Sun, Y., and Zhang, Q.: Primary and secondary organic aerosols in Fresno, California during wintertime: Results from high resolution aerosol mass spectrometry, Journal of Geophysical Research: Atmospheres, 117, n/a-n/a, 10.1029/2012jd018026, 2012.

Graham, B., Mayol-Bracero, O. L., Guyon, P., Roberts, G. C., Decesari, S., Facchini, M. C., Artaxo, P., Maenhaut, W., Koll, P., and Andreae, M. O.: Water-soluble organic compounds in biomass burning aerosols over Amazonia - 1. Characterization by NMR and GC-MS, J. Geophys. Res.-Atmos., 107, DOI:804710.801029/802001jd000336, 2002.

Guo, S., Hu, M., Zamora, M. L., Peng, J., Shang, D., Zheng, J., Du, Z., Wu, Z., Shao, M., Zeng, L., Molina, M. J., and Zhang, R.: Elucidating severe urban haze formation in China, Proceedings of the National Academy of Sciences of the United States of America, 111, 17373-17378,

10.1073/pnas.1419604111, 2014.
Halek, F., Nabi, G., and Kavousi, A.: Polycyclic aromatic hydrocarbons study and toxic equivalency factor (TEFs) in Tehran, IRAN, Environmental Monitoring and Assessment, 143, 303-311, 10.1007/s10661-007-9983-9, 2008.
Hallquist, M., Wenger, J. C., Baltensperger, U., Rudich, Y., Simpson, D., Claeys, M., Dommen, J., Donahue, N. M., George, C., Goldstein, A. H., Hamilton, J. F., Herrmann, H., Hoffmann, T., Iinuma, Y., Jang, M., Jenkin, M. E., Jimenez, J. L., Kiendler-Scharr, A., Maenhaut, W., McFiggans, G., Mentel, T. F., Monod, A., Prevot, A. S. H., Seinfeld, J. H., Surratt, J. D., Szmigielski, R., and Wildt, J.: The formation, properties and impact of secondary organic aerosol: current and emerging issues, Atmos. Chem. Phys., 9, 5155-5236, 2009.
Hays, M. D., Fine, P. M., Geron, C. D., Kleeman, M. J., and Gullett, B. K.: Open burning of agricultural biomass: Physical and chemical properties of particle-phase emissions, Atmos. Environ., 39, 6747-6764, https://doi.org/10.1016/j.atmosenv.2005.07.072, 2005.
Huang, R. J., Zhang, Y. L., Bozzetti, C., Ho, K. F., Cao, J. J., Han, Y. M., Daellenbach, K. R., Slowik, J. G., Platt, S. M., Canonaco, F., Zotter, P., Wolf, R., Pieber, S. M., Bruns, E. A., Crippa, M., Ciarelli, G., Piazzalunga, A., Schwikowski, M., Abbaszade, G., Schnelle-Kreis, J., Zimmermann, R., An, Z. S., Szidat, S., Baltensperger, U., El Haddad, I., and Prevot, A. S. H.: High secondary aerosol contribution to particulate pollution during haze events in China, Nature, 514, 218-222, 10.1038/nature13774, 2014.
Jaoui, M., Kleindienst, T. E., Lewandowski, M., Offenberg, J. H., and Edney, E. O.: Identification and quantification of aerosol polar oxygenated compounds bearing carboxylic or hydroxyl groups. 2. Organic tracer compounds from monoterpenes, Environ. Sci. Technol., 39, 5661-5673, 10.1021/es048111b, 2005.
Jaoui, M., Lewandowski, M., Kleindienst, T. E., Offenberg, J. H., and Edney, E. O.: β-caryophyllinic acid: An atmospheric tracer for β-caryophyllene secondary organic aerosol, Geophysical Research Letters, 34, doi:10.1029/2006GL028827, 2007.
Jenkin, M. E., Shallcross, D. E., and Harvey, J. N.: Development and application of a possible mechanism for the generation of cis -pinic acid from the ozonolysis of α - and β -pinene, Atmos. Environ., 34, 2837-2850, 2000.
Jimenez, J. L., Canagaratna, M. R., Donahue, N. M., Prevot, A. S. H., Zhang, Q., ., Kroll, J. H., Decarlo, P. F., Allan, J. D., Coe, H., ., and Ng, N. L.: Evolution of organic aerosols in the atmosphere, Science, 326, 1525-1529, 2009.
Kanakidou, M., Seinfeld, J. H., Pandis, S. N., Barnes, I., Dentener, F. J., Facchini, M. C., Van Dingenen, R., Ervens, B., Nenes, A., Nielsen, C. J., Swietlicki, E., Putaud, J. P., Balkanski, Y., Fuzzi, S., Horth, J., Moortgat, G. K., Winterhalter, R., Myhre, C. E. L., Tsigaridis, K., Vignati, E., Stephanou, E. G., and Wilson, J.: Organic aerosol and global climate modelling: a review, Atmos. Chem. Phys., 5, 1053-1123, 2005.
Kawamura, K., and Ikushima, K.: Seasonal changes in the distribution of dicarboxylic acids in the urban atmosphere, Environ. Sci. Technol., 27, 2227-2235, 1993.
Kawamura, K., Kosaka, M., and Sempere, R.: Distributions and seasonal changes in hydrocarbons in urban aerosols and rain waters, Chikyu Kagaku (Geochemistry), 29, 1-15 (In Japanese), 1995.
Kawamura, K., Ishimura, Y., and Yamazaki, K.: Four years' observations of terrestrial lipid class compounds in marine aerosols from the western North Pacific, Global Biogeochemical Cycles, 17, 10.1029/2001gb001810, 2003.
Kawamura, K., Imai, Y., and Barrie, L. A.: Photochemical production and loss of organic acids in high Arctic aerosols during long-range transport and polar sunrise ozone depletion events, Atmos. Environ., 39, 599-614, 10.1016/j.atmosenv.2004.10.020, 2005.
Kleindienst, T. E., Conver, T. S., McIver, C. D., and Edney, E. O.: Determination of secondary organic aerosol products from the photooxidation of toluene and their implications in ambient PM2.5, J. Atmos. Chem., 47, 79-100, 2004.
Kleindienst, T. E., Jaoui, M., Lewandowski, M., Offenberg, J. H., Lewis, C. W., Bhave, P. V., and Edney, E. O.: Estimates of the contributions of biogenic and anthropogenic hydrocarbons to secondary organic aerosol at a southeastern US location, Atmos. Environ., 41, 8288-8300, 10.1016/j.atmosenv.2007.06.045, 2007.
Kondo, Y., Miyazaki, Y., Takegawa, N., Miyakawa, T., Weber, R. J., Jimenez, J. L., Zhang, Q., and Worsnop, D. R.: Oxygenated and water-soluble organic aerosols in Tokyo, Journal of Geophysical Research, 112, doi: 10.1029/2006jd007056, 10.1029/2006jd007056, 2007.
Lelieveld, J., Evans, J. S., Fnais, M., Giannadaki, D., and Pozzer, A.: The contribution of outdoor air pollution sources to premature mortality on a global scale, Nature, 525, 367-371, 10.1038/nature15371, 2015.

Li, J. J., Wang, G. H., Cao, J. J., Wang, X. M., and Zhang, R. J.: Observation of biogenic secondary organic aerosols in the atmosphere of a mountain site in central China: temperature and relative humidity effects, Atmos. Chem. Phys., 13, 11535-11549, 10.5194/acp-13-11535-2013, 2013a.
Li, J. J., Wang, G. H., Wang, X. M., Cao, J. J., Sun, T., Cheng, C. L., Meng, J. J., Hu, T. F., and Liu, S. X.: Abundance, composition and source of atmospheric PM 2.5 at a remote site in the Tibetan Plateau, China, Tellus B, 65, doi:10.3402/tellusb.v3465i3400.20281, 2013b.
Li, J. J., Wang, G. H., Wu, C., Cao, C., Ren, Y. Q., Wang, J. Y., Li, J., Cao, J. J., Zeng, L. M., and Zhu, T.: Characterization of isoprene-derived secondary organic aerosols at a rural site in North China Plain with implications for anthropogenic pollution effects, Scientific reports, 8, DOI: 10.1038/s41598-41017-18983-41597, 10.1038/s41598-017-18983-7, 2018.
Li, W. J., Shao, L. Y., and Buseck, P. R.: Haze types in Beijing and the influence of agricultural biomass burning, Atmos. Chem. Phys., 10, 8119-8130, 10.5194/acp-10-8119-2010, 2010.
Li, X., Wang, S., Duan, L., Hao, J., and Nie, Y.: Carbonaceous Aerosol Emissions from Household Biofuel Combustion in China, Environ. Sci. Technol., 43, 6076-6081, 10.1021/es803330j, 2009.
Li, Y. J., Sun, Y., Zhang, Q., Li, X., Li, M., Zhou, Z., and Chan, C. K.: Real-time chemical characterization of atmospheric particulate matter in China: A review, Atmos. Environ., 158, 270-304, 10.1016/j.atmosenv.2017.02.027, 2017.
Li, Z. Q., Xia, X. G., Cribb, M., Mi, W., Holben, B., Wang, P. C., Chen, H. B., Tsay, S. C., Eck, T. F., Zhao, F. S., Dutton, E. G., and Dickerson, R. R.: Aerosol optical properties and their radiative effects in northern China, J. Geophys. Res.-Atmos., 112, 10.1029/2006jd007382, 2007.
Müller, L., Reinnig, M. C., Naumann, K. H., Saathoff, H., Mentel, T. F., Donahue, N. M., and Hoffmann, T.: Formation of 3-methyl-1,2,3-butanetricarboxylic acid via gas phase oxidation of pinonic acid – a mass spectrometric study of SOA aging, Atmos. Chem. Phys., 12, 1483-1496, 10.5194/acp-12-1483-2012, 2012.
Ma, Y., Russell, A. T., and Marston, G.: Mechanisms for the formation of secondary organic aerosol components from the gas-phase ozonolysis of alpha-pinene, Physical Chemistry Chemical Physics, 10, 4294-4312, 10.1039/b803283a, 2008.
Oros, D. R., and Simoneit, B. R. T.: Identification and emission rates of molecular tracers in coal smoke particulate matter, Fuel, 79, 515-536, http://dx.doi.org/10.1016/S0016-2361(99)00153-2, 2000.
Quan, J. N., Gao, Y., Zhang, Q., Tie, X. X., Cao, J. J., Han, S. Q., Meng, J. W., Chen, P. F., and Zhao, D. L.: Evolution of planetary boundary layer under different weather conditions, and its impact on aerosol concentrations, Particuology, 11, 34-40, 10.1016/j.partic.2012.04.005, 2013.
Rogge, W. F., Hildemann, L. M., Mazurek, M. A., Cass, G. R., and Simoneit, B. R. T.: Sources of Fine Organic Aerosols. 2. Noncatalyst and Catalyst-equipped Automobile and Heavy-duty Diesel Trucks, Environ. Sci. Technol., 27, 636-651, 1993a.
Rogge, W. F., Hildemann, L. M., Mazurek, M. A., Cass, G. R., and Simoneit, B. R. T.: Sources of Fine Organic Aerosols .4. Particulate Abrasion Products from Leaf Surfaces of Urban Plants, Environ. Sci. Technol., 27, 2700-2711, 1993b.
Shen, Z., Zhang, Q., Cao, J., Zhang, L., Lei, Y., Huang, Y., Huang, R. J., Gao, J., Zhao, Z., Zhu, C., Yin, X., Zheng, C., Xu, H., and Liu, S.: Optical properties and possible sources of brown carbon in PM 2.5 over Xi'an, China, Atmos. Environ., 150, 322-330, 10.1016/j.atmosenv.2016.11.024, 2017.
Simoneit, B. R. T., Schauer, J. J., Nolte, C. G., Oros, D. R., Elias, V. O., Fraser, M. P., Rogge, W. F., and Cass, G. R.: Levoglucosan, a tracer for cellulose in biomass burning and atmospheric particles, Atmos. Environ., 33, 173-182, 1999.
Simoneit, B. R. T.: Biomass burning - A review of organic tracers for smoke from incomplete combustion, Applied Geochemistry, 17, 129-162, 2002.
Simoneit, B. R. T., Elias, V. O., Kobayashi, M., Kawamura, K., Rushdi, A. I., Medeiros, P. M., Rogge, W. F., and Didyk, B. M.: Sugars - Dominant water-soluble organic compounds in soils and characterization as tracers in atmospheric particulate matter, Environ. Sci. Technol., 38, 5939-5949, 10.1021/es0403099, 2004a.
Simoneit, B. R. T., Kobayashi, M., Mochida, M., Kawamura, K., Lee, M., Lim, H. J., Turpin, B. J., and Komazaki, Y.: Composition and major sources of organic compounds of aerosol particulate matter sampled during the ACE-Asia campaign, J. Geophys. Res.-Atmos., 109, D19S10, 10.1029/2004jd004598, 2004b.
Sultan, C., Balaguer, P., Terouanne, B., Georget, V., Paris, F., Jeandel, C., Lumbroso, S., and Nicolas, J. C.: Environmental xenoestrogens, antiandrogens and disorders of male sexual differentiation, Molecular and Cellular Endocrinology, 178, 99-105, 10.1016/s0303-7207(01)00430-0, 2001.
Sun, Y. L., Jiang, Q., Wang, Z. F., Fu, P. Q., Li, J., Yang, T., and Yin, Y.: Investigation of the sources and evolution processes of severe haze pollution in Beijing in January 2013, J. Geophys. Res.-Atmos., 119, 4380-4398, 10.1002/2014jd021641, 2014.

Sun, Y. L., Jiang, Q., Xu, Y. S., Ma, Y., Zhang, Y. J., Liu, X. G., Li, W. J., Wang, F., Li, J., Wang, P. C., and Li, Z. Q.: Aerosol characterization over the North China Plain: Haze life cycle and biomass burning impacts in summer, J. Geophys. Res.-Atmos., 121, 2508-2521, 10.1002/2015jd024261, 2016.

Szmigielski, R., Surratt, J. D., Gomez-Gonzalez, Y., Van der Veken, P., Kourtchev, I., Vermeylen, R., Blockhuys, F., Jaoui, M., Kleindienst, T. E., Lewandowski, M., Offenberg, J. H., Edney, E. O., Seinfeld, J. H., Maenhaut, W., and Claeys, M.: 3-methyl-1,2,3-butanetricarboxylic acid: An atmospheric tracer for terpene secondary organic aerosol, Geophysical Research Letters, 34, L24811, 10.1029/2007gl031338, 2007.

Tian, J., Ni, H. Y., Cao, J. J., Han, Y. M., Wang, Q. Y., Wang, X. L., Chen, L. W. A., Chow, J. C., Watson, J. G., Wei, C., Sun, J., Zhang, T., and Huang, R. J.: Characteristics of carbonaceous particles from residential coal combustion and agricultural biomass burning in China, Atmospheric Pollution Research, 8, 521-527, 10.1016/j.apr.2016.12.006, 2017.

Tie, X. X., Huang, R. J., Dai, W. T., Cao, J. J., Long, X., Su, X. L., Zhao, S. Y., Wang, Q. Y., and Li, G. H.: Effect of heavy haze and aerosol pollution on rice and wheat productions in China, Scientific reports, 6, 10.1038/srep29612, 2016.

van Donkelaar, A., Martin, R. V., Brauer, M., Kahn, R., Levy, R., Verduzco, C., and Villeneuve, P. J.: Global Estimates of Ambient Fine Particulate Matter Concentrations from Satellite-Based Aerosol Optical Depth: Development and Application, Environmental Health Perspectives, 118, 847-855, 10.1289/ehp.0901623, 2010.

Venkataraman, C., Habib, G., Eiguren-Fernandez, A., Miguel, A. H., and Friedlander, S. K.: Residential biofuels in south Asia: Carbonaceous aerosol emissions and climate impacts, Science, 307, 1454-1456, 10.1126/science.1104359, 2005.

Wang, G. H., and Kawamura, K.: Molecular characteristics of urban organic aerosols from Nanjing: A case study of a mega-city in China, Environ. Sci. Technol., 39, 7430-7438, 10.1021/es051055+, 2005.

Wang, G. H., Kawamura, K., Lee, S., Ho, K. F., and Cao, J. J.: Molecular, seasonal, and spatial distributions of organic aerosols from fourteen Chinese cities, Environ. Sci. Technol., 40, 4619-4625, 10.1021/es060291x, 2006a.

Wang, G. H., Kawamura, K., Watanabe, T., Lee, S. C., Ho, K. F., and Cao, J. J.: High loadings and source strengths of organic aerosols in China, Geophysical Research Letters, 33, L2280110.1029/2006gl027624, 2006b.

Wang, G. H., Kawamura, K., Umemoto, N., Xie, M. J., Hu, S. Y., and Wang, Z. F.: Water-soluble organic compounds in PM2.5 and size-segregated aerosols over Mount Tai in North China Plain, J. Geophys. Res.-Atmos., 114, doi: 10.1029/2008jd011390, D1920810.1029/2008jd011390, 2009a.

Wang, G. H., Kawamura, K., Xie, M. J., Hu, S. Y., Cao, J. J., An, Z. S., Waston, J. G., and Chow, J. C.: Organic Molecular Compositions and Size Distributions of Chinese Summer and Autumn Aerosols from Nanjing: Characteristic Haze Event Caused by Wheat Straw Burning, Environ. Sci. Technol., 43, 6493-6499, 10.1021/es803086g, 2009b.

Wang, G. H., Chen, C. L., Li, J. J., Zhou, B. H., Xie, M. J., Hu, S. Y., Kawamura, K., and Chen, Y.: Molecular composition and size distribution of sugars, sugar-alcohols and carboxylic acids in airborne particles during a severe urban haze event caused by wheat straw burning, Atmos. Environ., 45, 2473-2479, 10.1016/j.atmosenv.2011.02.045, 2011.

Wang, G. H., Zhang, R. Y., Gomez, M. E., Yang, L. X., Zamora, M. L., Hu, M., Lin, Y., Peng, J. F., Guo, S., Meng, J. J., Li, J. J., Cheng, C. L., Hu, T. F., Ren, Y. Q., Wang, Y. S., Gao, J., Cao, J. J., An, Z. S., Zhou, W. J., Li, G. H., Wang, J. Y., Tian, P. F., Marrero-Ortiz, W., Secrest, J., Du, Z. F., Zheng, J., Shang, D. J., Zeng, L. M., Shao, M., Wang, W. G., Huang, Y., Wang, Y., Zhu, Y. J., Li, Y. X., Hu, J. X., Pan, B., Cai, L., Cheng, Y. T., Ji, Y. M., Zhang, F., Rosenfeld, D., Liss, P. S., Duce, R. A., Kolb, C. E., and Molina, M. J.: Persistent sulfate formation from London Fog to Chinese haze, Proceedings of the National Academy of Sciences of the United States of America, 113, 13630-13635, 10.1073/pnas.1616540113, 2016.

Xuan, Z., Renee C, M., Dan D, H., Nathan F, D., Bernard, A., Richard C, F., and John H, S.: Formation and evolution of molecular products in α-pinene secondary organic aerosol, Proceedings of the National Academy of Sciences of the United States of America, 112, 14168-14173, 2015.

Yang, Y. H., Chan, C. Y., Tao, J., Lin, M., Engling, G., Zhang, Z. S., Zhang, T., and Su, L.: Observation of elevated fungal tracers due to biomass burning in the Sichuan Basin at Chengdu City, China, Science of the Total Environment, 431, 68-77, 10.1016/j.scitotenv.2012.05.033, 2012.

Young, D. E., Kim, H., Parworth, C., Zhou, S., Zhang, X., Cappa, C. D., Seco, R., Kim, S., and Zhang, Q.: Influences of emission sources and meteorology on aerosol chemistry in a polluted urban environment: results from DISCOVER-AQ California, Atmos. Chem. Phys., 16, 5427-5451,

10.5194/acp-16-5427-2016, 2016.
Zhang, J. K., Cheng, M. T., Ji, D. S., Liu, Z. R., Hu, B., Sun, Y., and Wang, Y. S.: Characterization of submicron particles during biomass burning and coal combustion periods in Beijing, China, The Science of the total environment, 562, 812-821, 10.1016/j.scitotenv.2016.04.015, 2016.
Zhang, Q., Jimenez, J. L., Canagaratna, M. R., Allan, J. D., Coe, H., Ulbrich, I., Alfarra, M. R., Takami, A., Middlebrook, A. M., and Sun, Y. L.: Ubiquity and dominance of oxygenated species in organic aerosols in anthropogenically-influenced Northern Hemisphere midlatitudes, Geophysical Research Letters, 34, L13801, 2007a.
Zhang, Q., Streets, D. G., Carmichael, G. R., He, K. B., Huo, H., Kannari, A., Klimont, Z., Park, I. S., Reddy, S., Fu, J. S., Chen, D., Duan, L., Lei, Y., Wang, L. T., and Yao, Z. L.: Asian emissions in 2006 for the NASA INTEX-B mission, Atmos. Chem. Phys., 9, 5131-5153, 10.5194/acp-9-5131-2009, 2009.
Zhang, Y., Shao, M., Zhang, Y., Zeng, L., He, L., Zhu, B., Wei, Y., and Zhu, X.: Source profiles of particulate organic matters emitted from cereal straw burnings, Journal of Environmental Sciences, 19, 167-175, https://doi.org/10.1016/S1001-0742(07)60027-8, 2007b.
Zhu, Y., Yang, L., Chen, J., Wang, X., Xue, L., Sui, X., Wen, L., Xu, C., Yao, L., Zhang, J., Shao, M., Lu, S., and Wang, W.: Characteristics of ambient volatile organic compounds and the influence of biomass burning at a rural site in Northern China during summer 2013, Atmos. Environ., 124, 156-165, 10.1016/j.atmosenv.2015.08.097, 2016.

840 Table 1 Concentrations of carbonaceous components in the time-resolved (3-h) $PM_{2.5}$ samples in
841 the rural site of NCP during the whole sampling period, Period 1 (P1) and Period 2 (P2).

Component	Whole period (N=117)			Period 1 (N=28)			Period 2 (N=13)		
	Range	Mean	SD	Range	Mean	SD	Range	Mean	SD
$PM_{2.5}$ (μg m^{-3})	21~395	159	89	133~347	231	59	21~62	43	14
OC (μg m^{-3})	1.7~45.7	17.3	11.1	13.8~44.4	29.4	7.8	3.6~8.8	5.5	1.7
EC (μg m^{-3})	0.2~22.3	6.5	4.9	5.3~22.3	12.1	4.0	0.9~2.6	1.5	0.5
WSOC (μg m^{-3})	0.7~33.0	11.5	8.2	5.3~33.0	19.1	8.3	1.2~4.2	2.6	0.8
WIOC (μg m^{-3})	0.3~28.1	6.4	5.1	4.5~28.1	10.3	4.4	1.2~5.5	3.0	1.3
OC/EC	1.2~7.6	3.0	0.9	1.9~3.2	2.5	0.4	2.5~5.7	3.8	1.0
WSOC/OC	0.07~0.95	0.63	0.18	0.30~0.85	0.62	0.16	0.18~0.67	0.48	0.12
WIOC/OC	0.05~0.93	0.37	0.18	0.15~0.70	0.38	0.16	0.33~0.82	0.52	0.12

842
843
844

Table 2 Average concentrations of the organic compound classes (ng m^{-3}) in the time-resolved (3-h) $PM_{2.5}$ samples in the rural site of NCP during the whole study period, Period 1 (P1) and Period 2 (P2).

Compounds	Whole period (N=117)			Period 1 (N=28)			Period 2 (N=13)		
	Range	Mean	SD	Range	Mean	SD	Range	Mean	SD
n-Alkanes	9.97~722.2	206.9	149.3	94.7~722.3	343.7	134.1	25.1~103.2	54.3	22.4
CPI (C_{18}-C_{36})[a]	1.08~8.62	2.47	1.12	1.38~4.67	2.85	0.87	1.08~3.5	1.64	0.59
Fatty acids	64.6~1777	514.4	384.3	206.7~1528	900.3	358.3	81.4~234.4	145.3	47.7
CPI ($C_{21:0}$-$C_{30:0}$)[b]	2.26~9.15	4.24	1.14	3.49~6.11	4.21	0.64	2.26~8.57	3.50	1.64
Fatty alcohols	3.18~975.9	192.6	187.4	62.4~638.2	322.0	150.7	16.6~100.2	33.9	22.6
Sugar compounds	15.9~2228	432.8	428.9	151.9~1727	718.0	403.1	39.7~241.3	93.2	52.9
galactosan (G)	1.03~97.78	18.5	20.6	2.16~97.8	29.5	27.9	1.45~13.3	4.61	3.13
mannosan (M)	0.69~54.82	9.78	10.4	1.61~54.8	15.0	13.3	0.96~6.63	2.83	1.43
levoglucosan (L)	5.56~1447	240.1	287.8	29.3~1428	404.0	344.0	11.2~123	47.8	26.2
L/M ratio	4.03~71.8	22.8	8.85	13.9~71.8	29.7	12.2	11.3~23.1	18.0	4.28
L/(G+M) ratio	1.38~19.3	8.05	2.59	5.3~19.3	10.1	3.41	4.58~10.2	6.77	1.97
PAHs	1.11~48.5	12.0	11.0	4.21~37.7	18.6	11.0	1.25~5.01	2.33	0.98
Hopanes	0.66~10.81	3.46	2.38	0.86~9.97	4.40	2.48	1.14~2.28	1.81	0.31
Phthalate esters	17.7~219.9	84.9	41.3	68.8~183.1	111.5	32.7	31.5~100.8	51.1	18.1
Phthalic acids	17.1~487.2	154.5	93.9	91.3~388.6	211.0	87.1	17.1~81	46.3	17.1
Isoprene SOA tracers	11.1~404.1	111.9	85.8	48.3~404.1	208.5	104.9	34.8~127.5	57.0	29.4
Monoterpene SOA tracers	11.1~166.2	66.1	31.2	37.3~166.2	85.3	34.9	26.7~64.5	44.6	12.6
β-Caryophyllinic acid[c]	0.49~77.7	17.4	17.1	4.6~77.8	34.7	20.8	2.44~6.28	4.08	1.21
DHOPA[d]	1.59~35.3	9.36	7.15	4.06~35.3	15.6	9.80	2.7~6.99	4.16	1.42
Total measured organics	176.9~6249	1806	1308	843.3~5499	2973	1219	334.2~913.7	537.9	151.1
Total organics_C/OC[e] (%)	3.19~16.0	6.99	1.97	3.43~8.86	6.43	1.36	3.77~8.61	6.41	1.27

[a] CPI (C_{18}-C_{36}): carbon preference index for *n*-alkanes, (C_{19}+C_{21}+C_{23}+C_{25}+C_{27}+C_{29}+C_{31}+C_{33}+C_{35})/ (C_{18}+C_{20}+C_{22}+C_{24}+C_{26}+C_{28}+C_{30}+C_{32}+C_{34}).

[b] CPI ($C_{21:0}$-$C_{30:0}$): carbon preference index for fatty acids, ($C_{22:0}$+$C_{24:0}$+$C_{26:0}$+$C_{28:0}$+$C_{30:0}$)/ ($C_{21:0}$+$C_{23:0}$+$C_{25:0}$+$C_{27:0}$+$C_{29:0}$).

[c] *β*-Caryophyllinic acid: a tracer of *β*-caryophyllene-derived SOA.

[d] DHOPA: 2,3-dihydroxy-4-oxopentanoic acid, a tracer of toluene-derived SOA.

[e] All the quantified organic compounds were converted to their carbon contents to calculate the OC ratios.

Figure Captions

Figure 1. Backward trajectories of air masses (a,c) (provided by NOAA HYSPLIT modeling system, http://ready.arl.noaa.gov/HYSPLIT.php), and fire spots (b,d) (provided by Fire Information for Resource Management System, FIRMS, https://firms.modaps.eosdis.nasa.gov/firemap/), during Period 1 (P1) (Jun 13th 21:00-16th 15:00, 2013) and Period 2 (P2) (Jun 22nd 12:00-24th 06:00, 2013). Sampling site represented as purple star.

Figure 2. Temporal variations of $PM_{2.5}$, OC, EC, and WSOC during the whole sampling period. Shadows denote the two representative periods.

Figure 3. Linear correlations of OC with WSOC (a), levoglucosan with OC and WSOC(b).

Figure 4. Diurnal variation of OC/EC (a), WSOC/OC and levoglucosan/OC (b).

Figure 5. Temporal variations of ten organic compound classes detected in the summertime $PM_{2.5}$ samples at the rural site of NCP.

Figure 6. Temporal variations of organic tracers for biomass burning (a), and secondary products derived from *α*-/*β*-pinene (b-d), *β*-caryophyllene (e), and toluene (f).

Figure 7. Molecular distributions of *n*-alkanes (a and d), fatty acids (b and e), and fatty alcohols (c and f) in the $PM_{2.5}$ of the rural area.

Figure 8. Linear correlations of fatty acids (a), fatty alcohols (b), 3-hydroxyglutaric acid (c), and β-caryophyllinic acid (d) with levoglucosan.

Figure 9. Diurnal variation of the detected organic compound classes.

Figure 10. Diurnal variation of the SOA tracers derived from oxidation of *α*-/*β*-pinene (a-d), *β*-caryophyllene (e), and toluene (f).

Figure 11. A comparison of the average contributions of different sources-derived organics (converted to carbon content) to OC during P1 and P2.

Figure 12. Contributions (above) of primary organic carbon from biomass burning (OC_{bb}) and fungal spores (OC_{fp}), and secondary organic carbon from isoprene (SOC_i), *α*-/*β*-pinene (SOC_p), *β*-caryophyllene (SOC_p), and toluene (SOC_t) to OC in the time-resolved (3 h) rural aerosols, and their relative abundances (down). All the contributions were estimated by tracer-based method.

Figure 13. Average contributions of direct emissions from biomass burning (BB) and fungal spores (OC_{fp}), secondary oxidation from isoprene (SOC_i), *α*-/*β*-pinene (SOC_p),*β*-caryophyllene (SOC_p), and toluene (SOC_t) to OC in P1 and P2. All the contributions were estimated by tracer-based method.

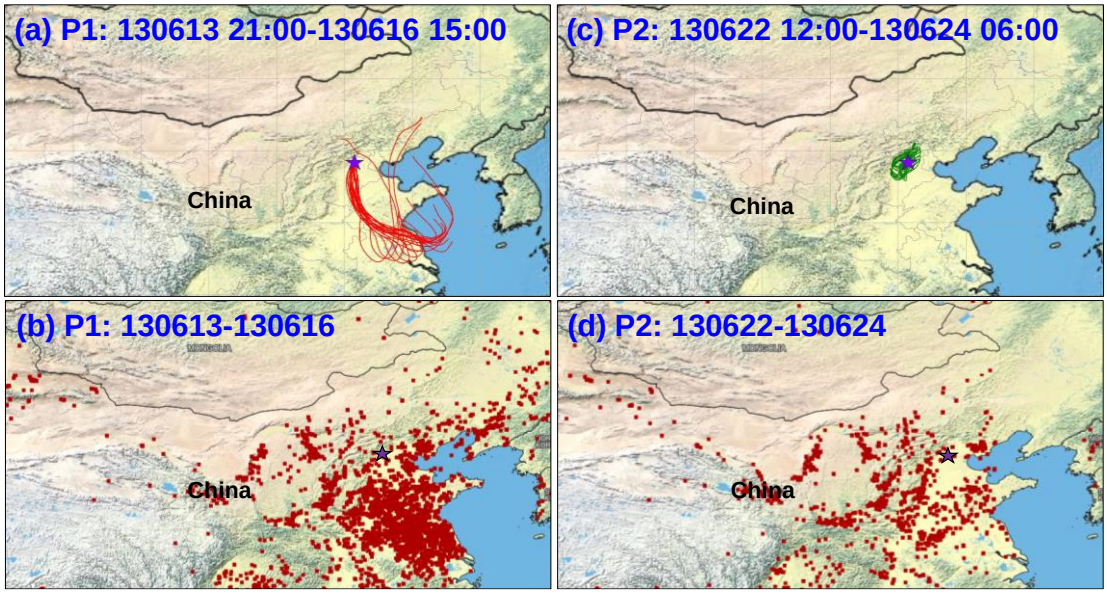

Figure 1. Backward trajectories of air masses (a,c) (provided by NOAA HYSPLIT modeling system, http://ready.arl.noaa.gov/HYSPLIT.php), and fire spots (b,d) (provided by Fire Information for Resource Management System, FIRMS, https://firms.modaps.eosdis.nasa.gov/firemap/), during Period 1 (P1) (Jun 13th 21:00-16th 15:00, 2013) and Period 2 (P2) (Jun 22nd 12:00-24th 06:00, 2013). Sampling site represented as purple star.

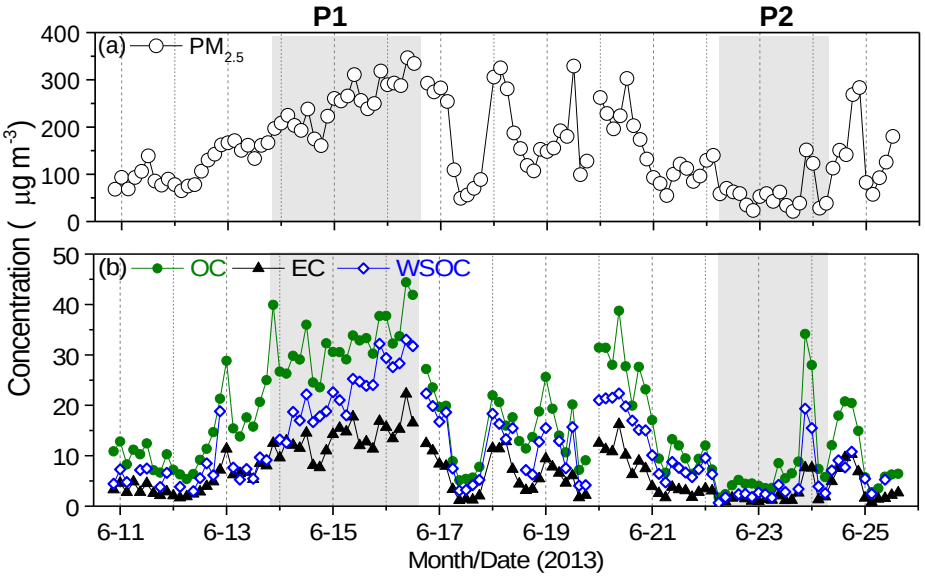

Figure 2. Temporal variations of $PM_{2.5}$, OC, EC, and WSOC during the whole sampling period. Shadows denote the two representative periods.

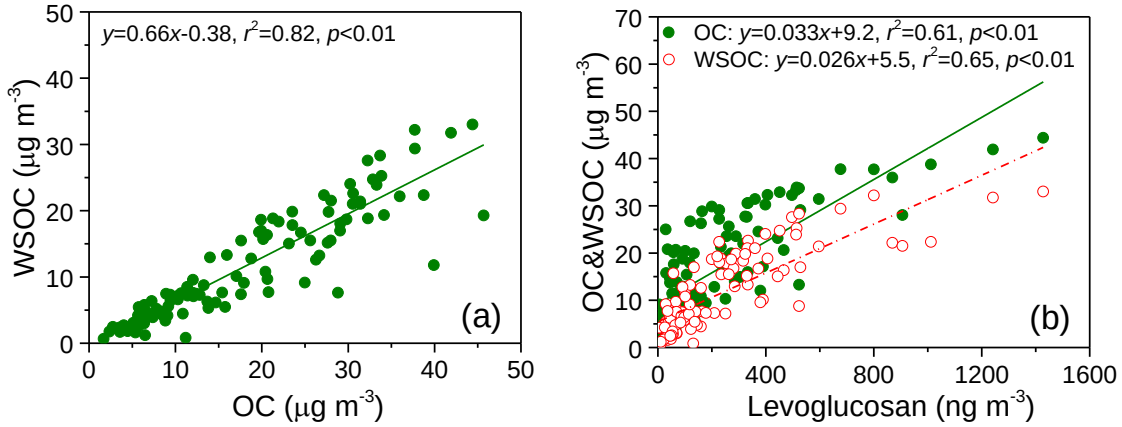

Figure 3. Linear correlations of OC with WSOC (a), levoglucosan with OC and WSOC(b).

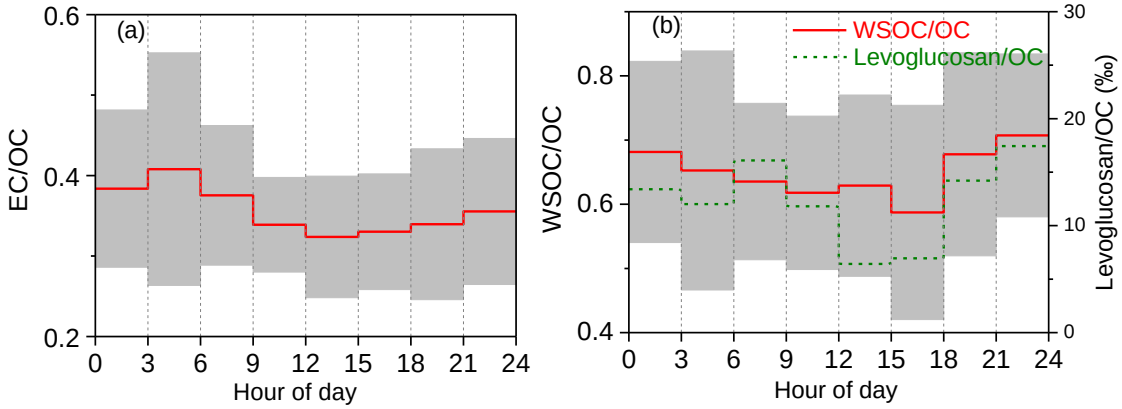

Figure 4. Diurnal variation of OC/EC (a), WSOC/OC and levoglucosan/OC (b).

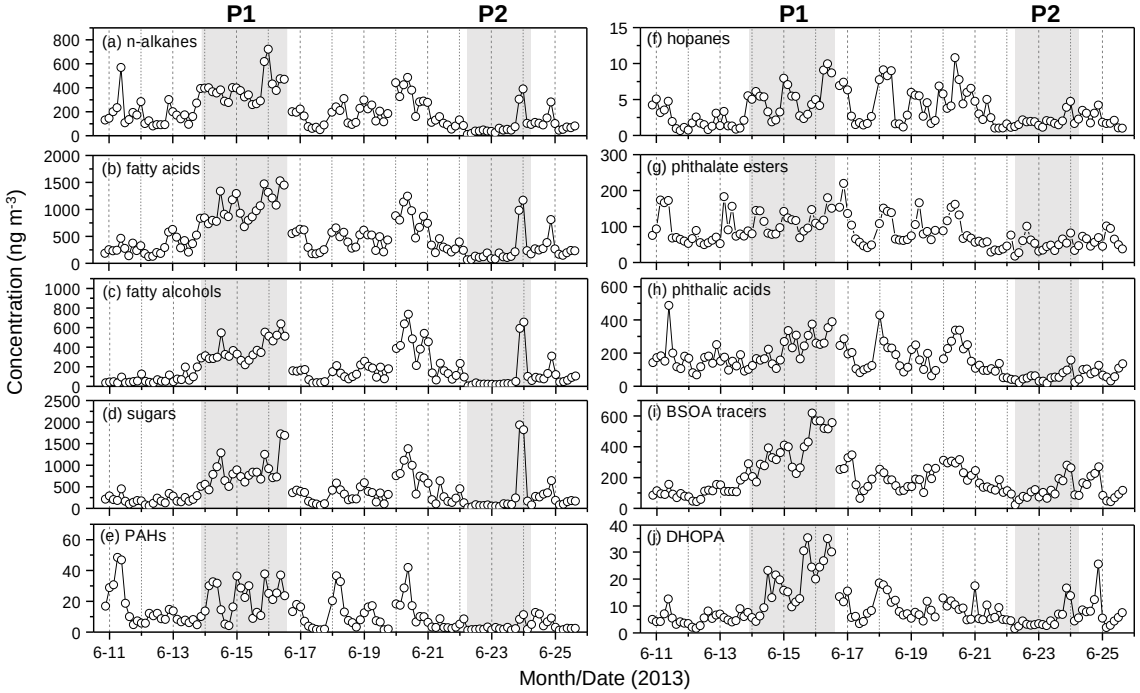

915

916 Figure 5. Temporal variations of ten organic compound classes detected in the summertime $PM_{2.5}$
917 samples at the rural site of NCP.

918

919

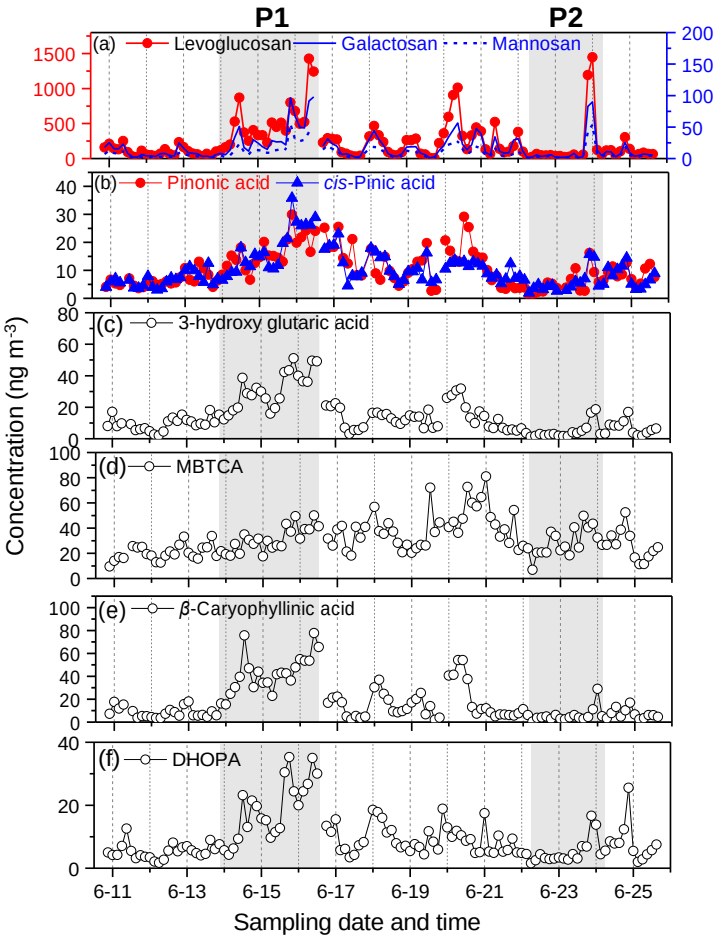

Figure 6. Temporal variations of organic tracers for biomass burning (a), and secondary products derived from *α*-/*β*-pinene (b-d), *β*-caryophyllene (e), and toluene (f).

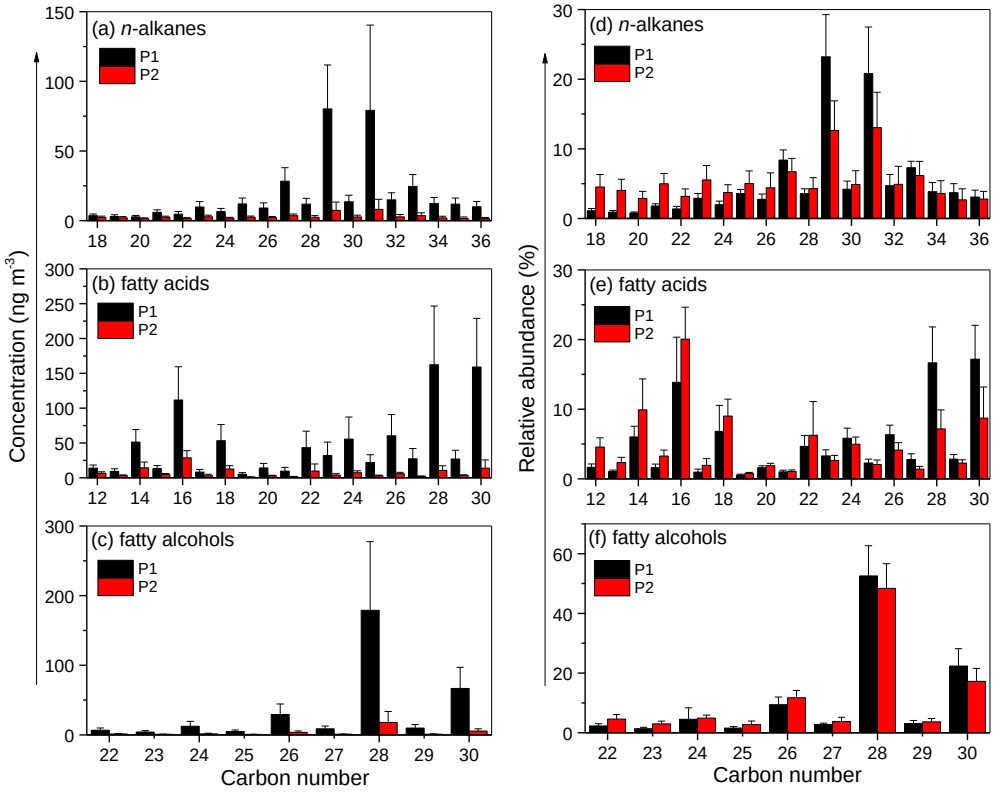

924

925 Figure 7. Molecular distributions of *n*-alkanes (a and d), fatty acids (b and e), and fatty alcohols (c and
926 f) in the $PM_{2.5}$ of the rural area.

927

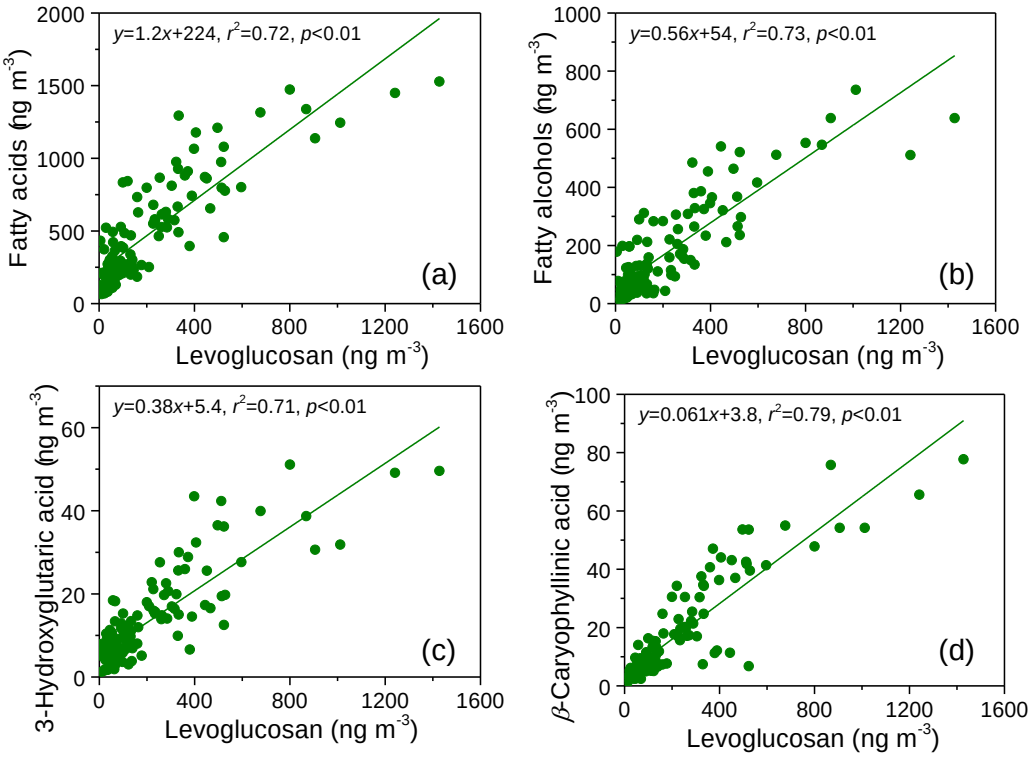

928

929 Figure 8. Linear correlations of fatty acids (a), fatty alcohols (b), 3-hydroxyglutaric acid (c), and β-
930 caryophyllinic acid (d) with levoglucosan.

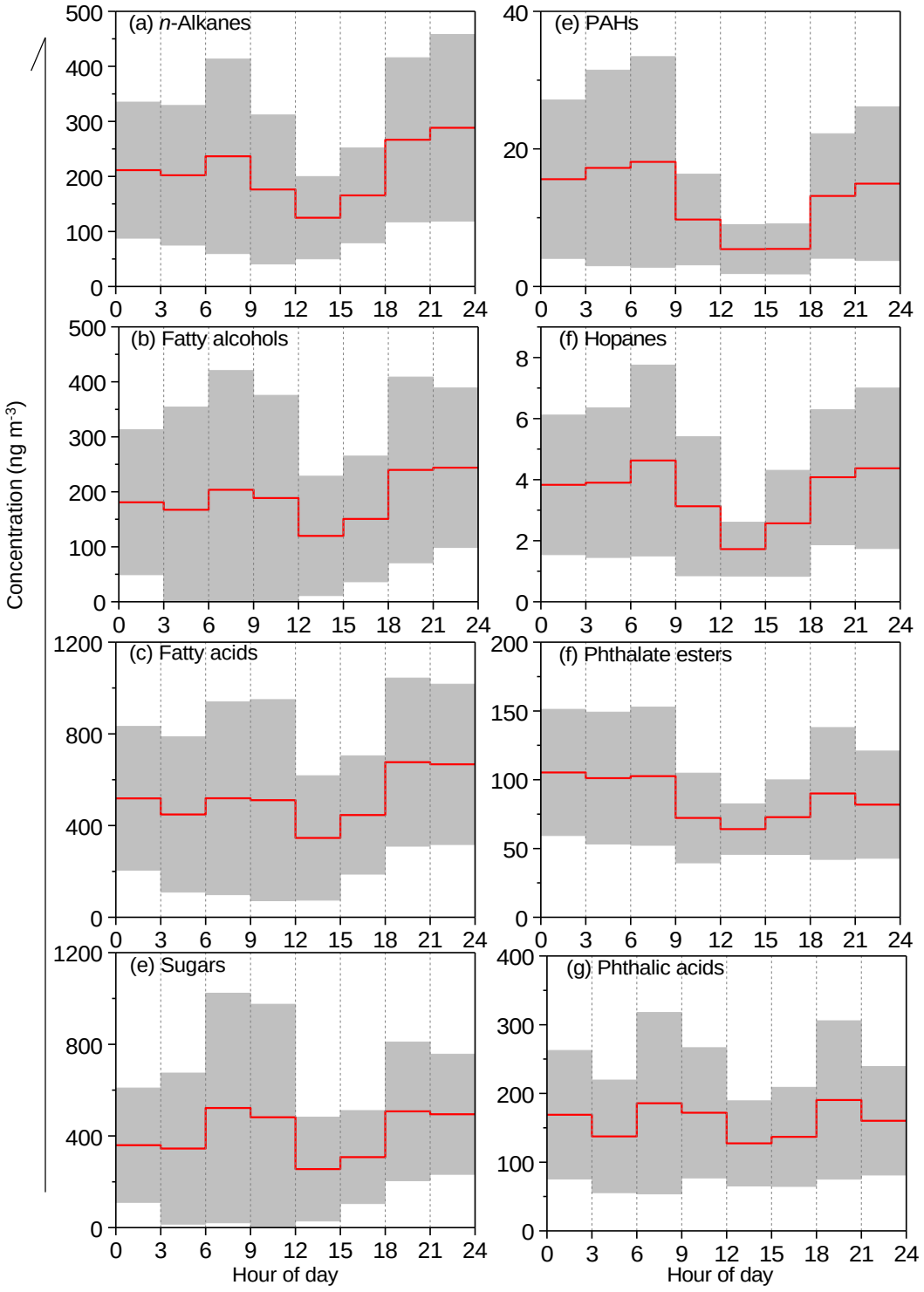

Figure 9. Diurnal variation of the detected organic compound classes.

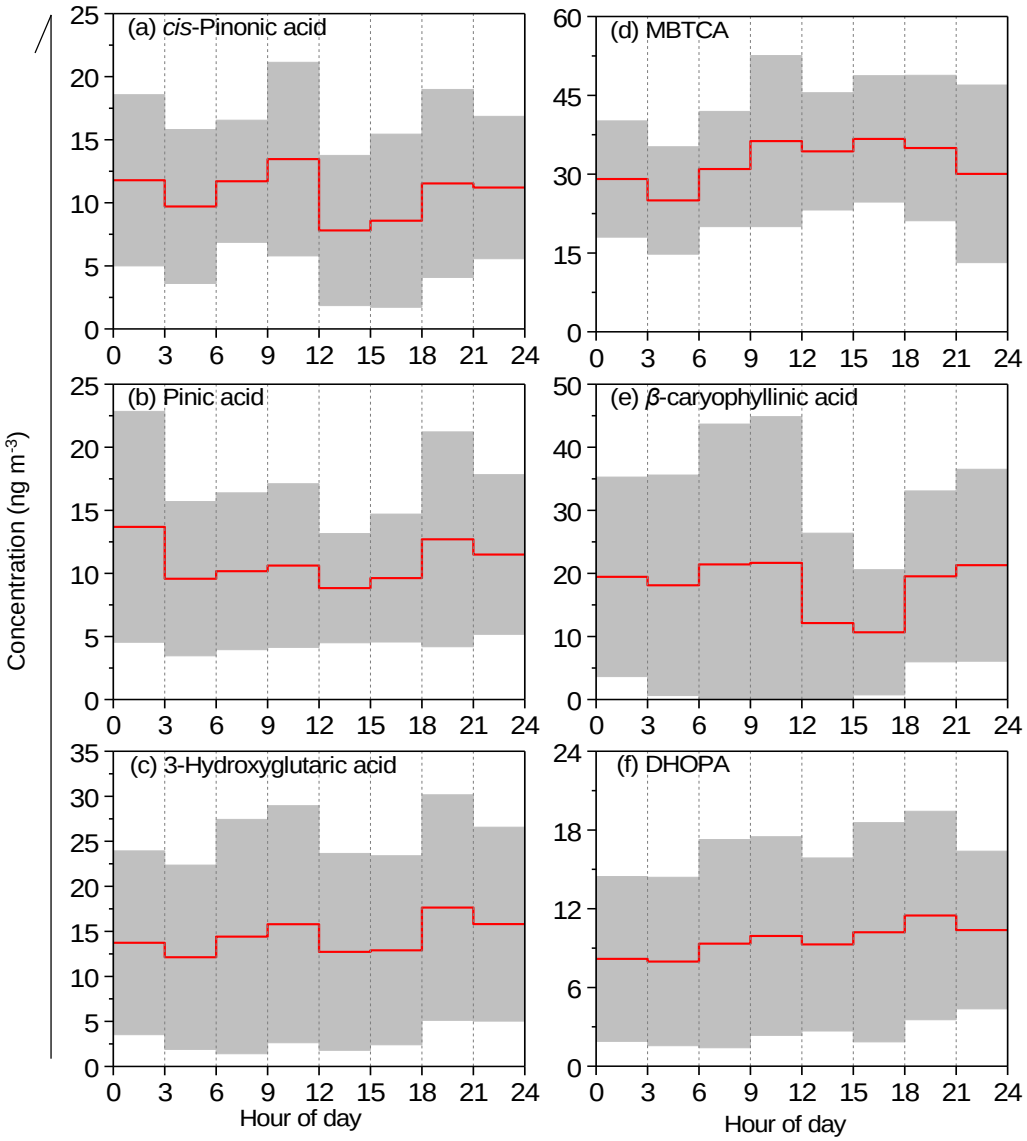

Figure 10. Diurnal variation of the SOA tracers derived from oxidation of *α*-/*β*-pinene (a-d), *β*-caryophyllene (e), and toluene (f).

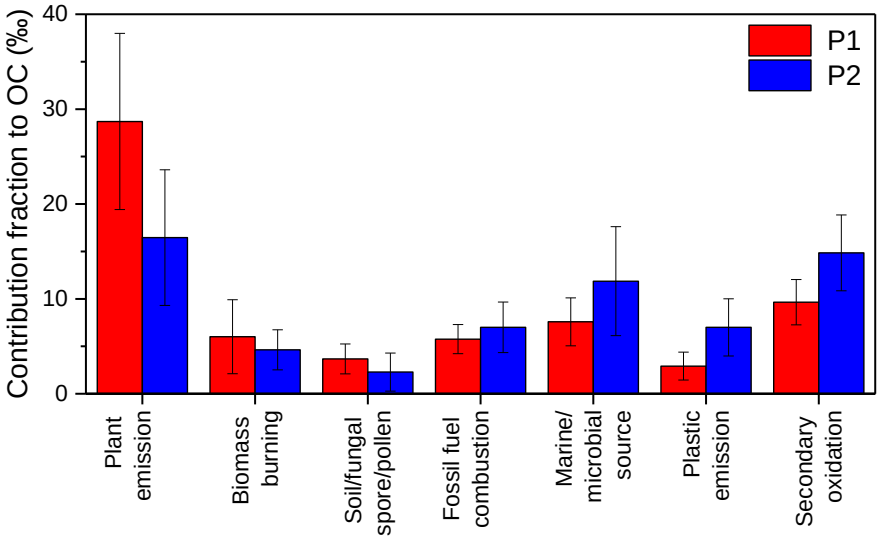

Figure 11 A comparison of the average contributions of different sources-derived organics (converted to carbon content) to OC during P1 and P2.

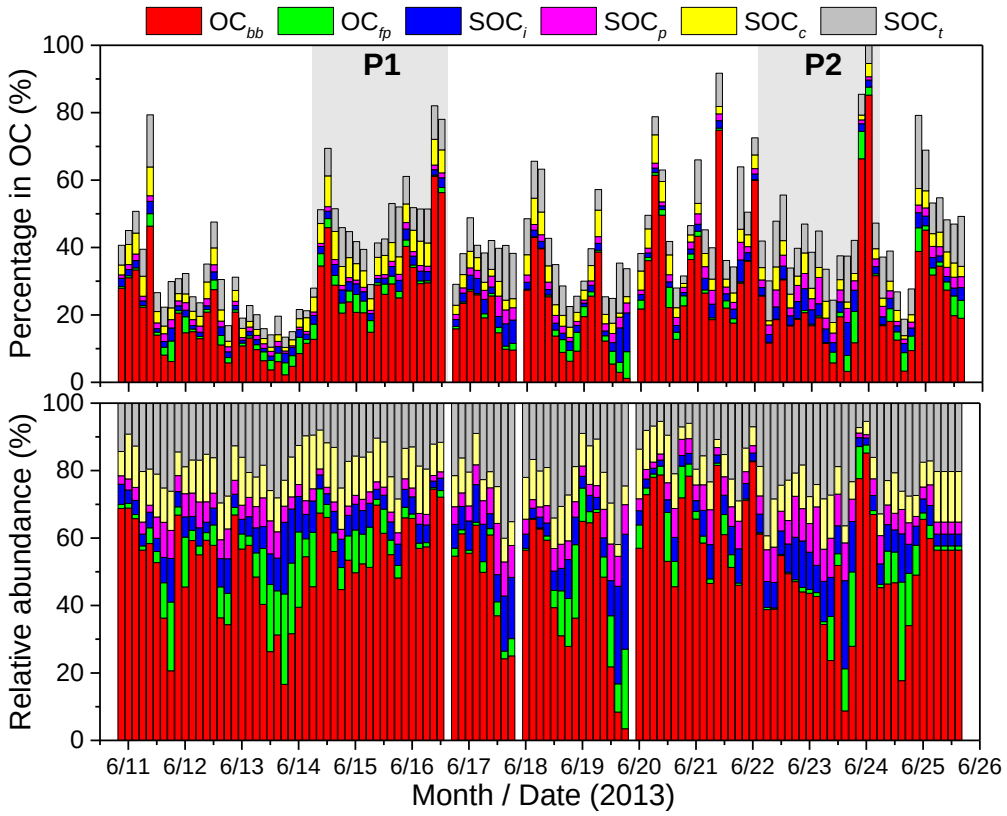

Figure 12. Contributions (above) of primary organic carbon from biomass burning (OC_{bb}) and fungal spores (OC_{fp}), and secondary organic carbon from isoprene (SOC_i), *α*-/*β*-pinene (SOC_p), *β*-caryophyllene (SOC_p), and toluene (SOC_t) to OC in the time-resolved (3 h) rural aerosols, and their relative abundances (down). All the contributions were estimated by tracer-based method.

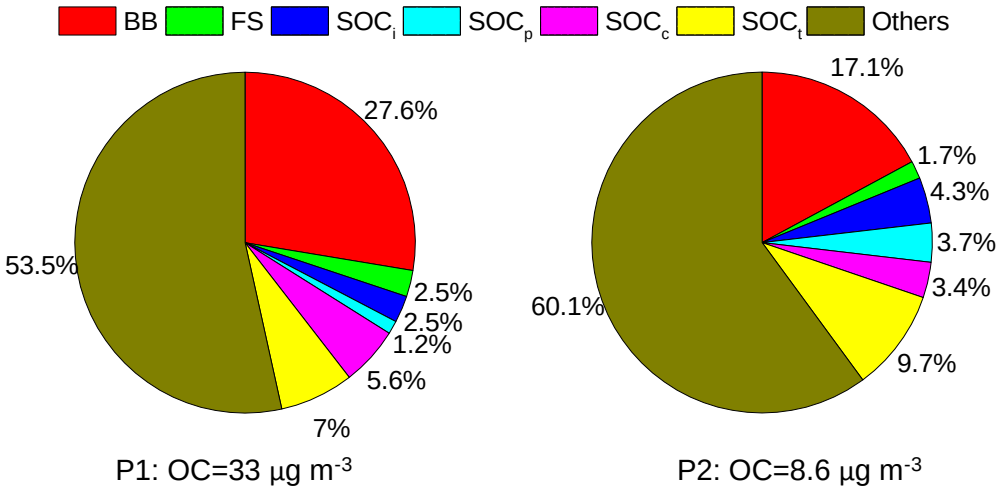

Figure 13. Average contributions of direct emissions from biomass burning (BB) and fungal spores (OC_{fp}), secondary oxidation from isoprene (SOC_i), *α-/β*-pinene (SOC_p),*β*-caryophyllene (SOC_p), and toluene (SOC_t) to OC in P1 and P2. All the contributions were estimated by tracer-based method.